Structures Research
Report 2018/127208

University of Florida
Civil and Coastal Engineering

UF

University of Florida
Civil and Coastal Engineering

Final Report **JUNE 2018**

Wind Effects on Mast Arms

Principal investigator:
Jennifer A. Bridge, Ph.D.

Co-Principal investigators:
Gary R. Consolazio, Ph.D.
Kurtis R. Gurley, Ph.D.

Research assistants:
Neandro J. DeMello
Joshua Smith

Department of Civil and Coastal Engineering
University of Florida
P.O. Box 116580
Gainesville, Florida 32611

Sponsor:
Florida Department of Transportation (FDOT)
Christina Freeman, P.E. – Project Manager
Alan El-Urfali, P.E. – Co-Project Manager

Contract:
FDOT Contract No. BDV31-977-59
UF Project Nos. 127208

DISCLAIMER

The opinions, findings, and conclusions expressed in this publication are those of the authors and not necessarily those of the State of Florida Department of Transportation.

SI* (MODERN METRIC) CONVERSION FACTORS

*APPROXIMATE CONVERSIONS **TO** SI UNITS*

SYMBOL	WHEN YOU KNOW	MULTIPLY BY	TO FIND	SYMBOL
LENGTH				
in	inches	25.4	millimeters	mm
ft	feet	0.305	meters	m
yd	yards	0.914	meters	m
mi	miles	1.61	kilometers	km
AREA				
in^2	square inches	645.2	square millimeters	mm^2
ft^2	square feet	0.093	square meters	m^2
yd^2	square yard	0.836	square meters	m^2
ac	acres	0.405	hectares	ha
mi^2	square miles	2.59	square kilometers	km^2
VOLUME				
fl oz	fluid ounces	29.57	milliliters	mL
gal	gallons	3.785	liters	L
ft^3	cubic feet	0.028	cubic meters	m^3
yd^3	cubic yards	0.765	cubic meters	m^3
NOTE: volumes greater than 1000 L shall be shown in m^3				
MASS				
oz	ounces	28.35	grams	g
lb	pounds	0.454	kilograms	kg
T	short tons (2,000 lb)	0.907	Megagrams	Mg (or "t")
TEMPERATURE (exact degrees)				
ºF	Fahrenheit	5(F-32)/9 or (F-32)/1.8	Celsius	ºC
FORCE and PRESSURE or STRESS				
kip	1,000 pound force	4.45	kilonewtons	kN
lbf	pound force	4.45	newtons	N
lbf/in^2	pound force per square inch	6.89	kilopascals	kPa
ksi	kips force per square inch	6.89	Megapascals	MPa

*SI is the symbol for the International System of Units. Appropriate rounding should be made to comply with Section 4 of ASTM E380.

SI* (MODERN METRIC) CONVERSION FACTORS

*APPROXIMATE CONVERSIONS **FROM** SI UNITS*

SYMBOL	WHEN YOU KNOW	MULTIPLY BY	TO FIND	SYMBOL
LENGTH				
mm	millimeters	0.039	inches	in
m	meters	3.28	feet	ft
m	meters	1.09	yards	yd
km	kilometers	0.621	miles	mi
AREA				
mm^2	square millimeters	0.0016	square inches	in^2
m^2	square meters	10.764	square feet	ft^2
m^2	square meters	1.195	square yards	yd^2
ha	hectares	2.47	acres	ac
km^2	square kilometers	0.386	square miles	mi^2
VOLUME				
mL	milliliters	0.034	fluid ounces	fl oz
L	liters	0.264	gallons	gal
m^3	cubic meters	35.314	cubic feet	ft^3
m^3	cubic meters	1.307	cubic yards	yd^3
MASS				
g	grams	0.035	ounces	oz
kg	kilograms	2.202	pounds	lb
Mg (or "t")	megagrams (or "metric ton")	1.103	short tons (2000 lb)	T
TEMPERATURE (exact degrees)				
ºC	Celsius	1.8C+32	Fahrenheit	ºF
ILLUMINATION				
lx	lux	0.0929	foot-candles	fc
cd/m^2	candela/m^2	0.2919	foot-Lamberts	fl
FORCE and PRESSURE or STRESS				
kN	kilonewtons	0.225	1000 pound force	kip
N	newtons	0.225	pound force	lbf
kPa	kilopascals	0.145	pound force per square inch	lbf/in^2

*SI is the symbol for the International System of Units. Appropriate rounding should be made to comply with Section 4 of ASTM E380.

TECHNICAL REPORT DOCUMENTATION PAGE

1. Report No.	2. Government Accession No.	3. Recipient's Catalog No.

4. Title and Subtitle	5. Report Date
Wind Effects on Mast Arms	June 2018
	6. Performing Organization Code
	8. Performing Organization Report No.
7. Author(s) Jennifer Bridge, Gary Consolazio, Kurtis Gurley, Neandro DeMello, Joshua Smith	2018/127208
9. Performing Organization Name and Address University of Florida Department of Civil and Coastal Engineering 365 Weil Hall, P.O. Box 116580 Gainesville, FL 32611-6580	10. Work Unit No. (TRAIS)
	11. Contract or Grant No. BDV31-977-59
12. Sponsoring Agency Name and Address Florida Department of Transportation Research Management Center 605 Suwannee Street, MS 30 Tallahassee, FL 32399-0450	13. Type of Report and Period Covered Final Report; June 2016 through June 2018
	14. Sponsoring Agency Code

15. Supplementary Notes

16. Abstract

In this study, current procedures employed by the FDOT for analysis and design of mast arm structures were reviewed, and experiments were conducted to identify residual mast arm system capacity. A collection of nine mast arm configurations was selected to represent mast arm designs commonly used in Florida, as well as those most often identified as being 'at capacity', based on the current design and analysis procedures. Findings from review and experimental testing indicated that selected parameters—Height and Exposure Factor, K_Z, and Drag Coefficient, C_d (specifically those applied to segments of the mast arm shielded by signals or signs)—used for wind-load calculations may be conservative.

It was concluded that height-dependent calculations of K_Z, as opposed to the current calculation using a fixed height of 24.4 feet, could yield lower K_Z values, and therefore lower the design wind loads on the mast arm. Furthermore, experimental wind tunnel tests conducted in this study identified that load-reducing shielding (aerodynamic shielding) of the mast arm does occur. This report proposes that the reduced wind load on the mast arm segments shielded by an attachment be implemented in design load calculations by reducing the drag coefficient on the attachment while continuing to fully load the mast arm as if unshielded. This reduced attachment drag coefficient is referred to as an incremental drag coefficient (C_{di}). In addition to design load parameter modifications, hardware modifications (denoted Enclosed and Slotted) were developed and experimentally tested. Results from experimental testing of the Enclosed modification demonstrated that the addition of covers provided no load reduction compared to unmodified attachments. Results for the Slotted modification showed that a reduction in the projected area of the back plate yielded a proportional reduction in loads on the attachment. However, field implementation of area reduction (folding, rotating or mesh panels) will require full-scale testing to quantify the load reduction proportionality constant.

17. Key Words	18. Distribution Statement
Mast-arm; static wind load design; drag coefficient	No restrictions.

19. Security Classif. (of this report)	20. Security Classif. (of this page)	21. No. of Pages	22. Price
Unclassified	Unclassified	83	

Form DOT F 1700.7 (8-72). Reproduction of completed page authorized

EXECUTIVE SUMMARY

In this study, current procedures employed by the FDOT for analysis and design of mast arm structures were reviewed, and experiments were conducted to identify residual mast arm system capacity. A collection of nine mast arm configurations was selected to represent mast arm designs commonly used in Florida, as well as those most often identified as being 'at capacity', based on the current design and analysis procedures. Findings from review and experimental testing indicated that selected parameters—Height and Exposure Factor, K_Z, and Drag Coefficient, C_d (specifically those applied to segments of the mast arm shielded by signals or signs)—used for wind-load calculations may be conservative.

It was concluded that height-dependent calculations of K_Z, as opposed to the current calculation using a fixed height of 24.4 feet, could yield lower K_Z values, and therefore lower the design wind loads on the mast arm. Furthermore, experimental wind tunnel tests conducted in this study identified that load-reducing shielding (aerodynamic shielding) of the mast arm does occur. This report proposes that the reduced wind load on the mast arm segments shielded by an attachment be implemented in design load calculations by reducing the drag coefficient on the attachment while continuing to fully load the mast arm as if unshielded. This reduced attachment drag coefficient is referred to as an incremental drag coefficient (C_{di}). In addition to design load parameter modifications, hardware modifications (denoted Enclosed and Slotted) were developed and experimentally tested. Results from experimental testing of the Enclosed modification demonstrated that the addition of covers provided no load reduction compared to unmodified attachments. Results for the Slotted modification showed that a reduction in the projected area of the back plate yielded a proportional reduction in loads on the attachment. However, field implementation of area reduction (folding, rotating or mesh panels) will require full-scale testing to quantify load reduction proportionality constant.

TABLE OF CONTENTS

LIST OF FIGURES

Figure Page

LIST OF TABLES

Table Page

1. Introduction

Mast arm structures with cantilevered arms are known to be wind-sensitive structures. Previously, research on mast arm structures has primarily focused on vibrations and fatigue analysis under dynamic wind loading conditions (Chen et al., 2001; Zuo and Letchford, 2010; Pulipakaa et al. 1998; Letchford and Cruzado, 2008). The focus of this study is static wind loading of mast arm structures. Based on current Florida Department of Transportation (FDOT) static wind load analysis procedures and design specifications, a significant fraction of the existing inventory of mast arm structures in the State of Florida are at maximum capacity with regard to supporting traffic signals and signs. As a result, additional traffic or safety-related hardware cannot be added without changes to or replacement of such structures. The primary objective of this research project is to investigate whether additional residual capacity can be identified in order to increase the quantity of traffic-related hardware components (e.g., signs, traffic signals, safety equipment) that can safely be attached to mast arm structures without necessitating overall structural replacement. There are two approaches that would potentially allow additional hardware installation without replacing the existing structures: (1) determine whether current static wind load analysis methods and design specifications used by the FDOT for mast arms are overly conservative, and (2) design and experimentally test hardware modifications that could reduce aerodynamic drag and/or projected area, thereby reducing the overall wind loads.

Structural assessment methods currently implemented by the FDOT for purposes of evaluating mast arm structural adequacy under wind loading conditions conservatively assume that global wind-induced forces can be computed by summing (superimposing) the effects of individual wind forces acting on each component (upright pole, mast arm, signs, signals, etc.). Under this assumption, the design wind pressure (P_Z) and wind-induced force (F) for each component are computed and then used in an overall static structural analysis of the mast arm system.

Determination of wind-induced loading on mast arm structures begins with the calculation of design wind pressure. According to AASHTO LRFD LTS-1 (2015), P_Z is computed as:

$$P_Z = 0.00256 \times K_Z \times K_d \times G \times V^2 \times C_d \quad (1)$$

where z is the height, K_Z is the 'height and exposure factor', G is the 'gust effect factor', V is the 'design wind speed', K_d is the 'directionality factor', and C_d is the 'drag coefficient'. The values of wind coefficients (i.e., drag coefficient, height and exposure factor, and gust effect factor) currently employed by FDOT are approximations drawn from relevant literature or design specifications. Once P_Z is calculated, the wind-induced force (F) acting on each mast arm component is computed as the product of design wind pressure and projected area (A):

$$F = P_Z \times A \quad (2)$$

Component wind forces, and therefore global wind reactions, are strongly influenced by the drag coefficients C_d assigned to each component. However, additional investigation was needed to understand how wind forces are influenced when two objects, such as signal and mast arm pole, are in close proximity.

Under the design approach of superimposing wind-induced forces, the phenomenon of aerodynamic 'shielding' is conservatively neglected in the current FDOT structural assessment methods. Aerodynamic shielding occurs when two objects in a flow field are located in close

enough proximity that flow around one (e.g., a traffic signal or sign face) disrupts flow around the other (e.g., an arm pole). In such a scenario, the downwind object is said to be 'shielded' (at least partially) by the upwind object. As a result, the downwind object is typically subjected to a drag force smaller in magnitude than that which would be produced if the same object were placed in the flow field by itself. In conditions involving shielding, the overall (i.e., 'effective') drag force acting on the two objects in question (upwind and downwind) is smaller in magnitude than the simple summation of drag forces computed individually for each object. Harper et al. (2016), Consolazio et al. (2013), and Consolazio and Edwards (2014) showed that aerodynamic shielding arising from interference between adjacent bridge girders affects drag coefficients of shielded girders. Zdravkovich and Pridden (1977) studied flow around two circular cylinders in series (i.e., back-to-back) and found that the drag coefficient on the shielded cylinder varied with distance between cylinders. For mast arms, where signals are in close proximity to the supporting arm, wind-induced forces acting on the 'global' system—i.e. a mast arm combined with attachments (sign panels, signals, etc.)—are less than those computed by a simple superposition of individual force effects. Quantification of this phenomenon would be an example of identifying residual capacity.

This report presents findings from experimental testing and analytical evaluation of representative mast arm structures and currently employed wind coefficients. Section 2 provides an overview of the currently employed FDOT MathCAD program used to analyze and design mast arm structures. Section 2 also introduces the selection of representative mast arm structures, as well as processes and procedures used to experimentally and analytically evaluate them. Section 3 reviews selected parameters from the MathCAD program that may affect the computed capacity of mast arm structures. Additionally, it includes an investigation into the selection of drag coefficients based on previous research and through wind tunnel testing. In Section 4, modifications are proposed to selected parameters that were found to have a significant impact on important structural demands (i.e., global wind reactions). The influence of implementing the proposed modifications are also presented in this section. Section 5 provides hardware modifications that could potentially reduce wind loading, and the theoretical load reduction mechanism associated with each proposed modification. In Section 6, the performance of selected hardware modifications is studied through wind tunnel testing, as well as through implementation in the FDOT MathCAD program. Section 7 provides concluding remarks and recommendations.

2. Development of Process and Procedures for Evaluation of Mast Arm Structures

This section provides an overview of the MathCAD program that is currently employed by FDOT in design and analysis of mast arm structures, and a discussion of the procedure for reviewing design parameters that may affect global wind load reactions. A collection of representative mast arm structures are introduced, as are general processes and procedures that were used to experimentally and analytically examine these structures.

2.1. Overview

Currently FDOT engineers use a MathCAD program (FDOT Mast Arm LRFD v1.0) to analyze and design mast arm structures in accordance with AASHTO LRFD LTS-1 (2015) and the FDOT Structures Manual (2017). Input data required by the program includes mast arm and traffic control hardware information such as dimensional data, hardware locations and sizes, and design wind speed. Structural analysis calculations are performed for main structural components as well as for connections. Loads considered in the structural analysis include dead load and wind load. The worksheet consists of several distinct analysis modules:

- Mast Arm 1 / Mast Arm 2
- Luminaire
- Upright
- Mast Arm Connections
- Base Plate Analysis
- Foundation Analysis
- Fatigue Analysis

Modules relevant to the steel mast arm components and global force reactions were reviewed for appropriate interpretation and application of design requirements (AASHTO, FDOT) with particular attention given to the ultimate wind load case. In Section 1, drag coefficients were identified as critical design parameters that affect global wind load reactions. Drag coefficients used in the FDOT program and corresponding values published in the literature are compared. Additional structural parameters that affect computed mast arm capacity are also discussed. Following a review of the FDOT MathCAD program, experimental wind tunnel tests were conducted to further study the potential effects of aerodynamic shielding. These experimental tests were conducted using representative mast arm structures that were selected in coordination with FDOT.

2.2. Selection of Representative Mast Arm Structures

A collection of mast arm configurations was selected to represent mast arm designs commonly used in Florida, as well as those most often identified as being ‘at capacity’ based on the current design and analysis methodologies. In coordination with the FDOT, nine basic structural configurations were selected for analysis and testing. Figure 2-1 – Figure 2-9 show dimensions and specified design standards for the selected representative mast arms. Each of the selected mast arm structures utilize 12-sided polygonal (dodecagonal) cylinders with a diameter taper of 0.14-inch-per-foot. Critical parameters that varied among the selected mast arms included:

- Arm type (diameter)
- Pole type (diameter)
- Arm length
- Pole height
- Quantity of traffic signals and signs
- Signal orientation (horizontal, vertical)
- Signal back plates (present, absent)
- Design standard (FDOT, Miami-Dade; various years)

Structures representative of the Miami-Dade area (Figure 2-1, Figure 2-2, Figure 2-5, Figure 2-6, Figure 2-7, and Figure 2-9) utilize horizontal signals. The remaining structures (Figure 2-3, Figure 2-4, and Figure 2-8) primarily utilize vertical signals, but horizontal configurations were also considered.

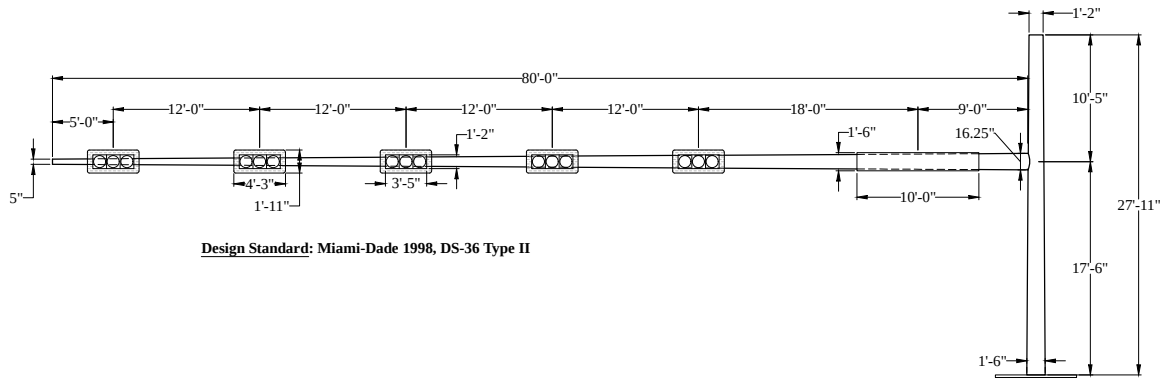

Figure 2-1. Representative FDOT Mast Arm 1

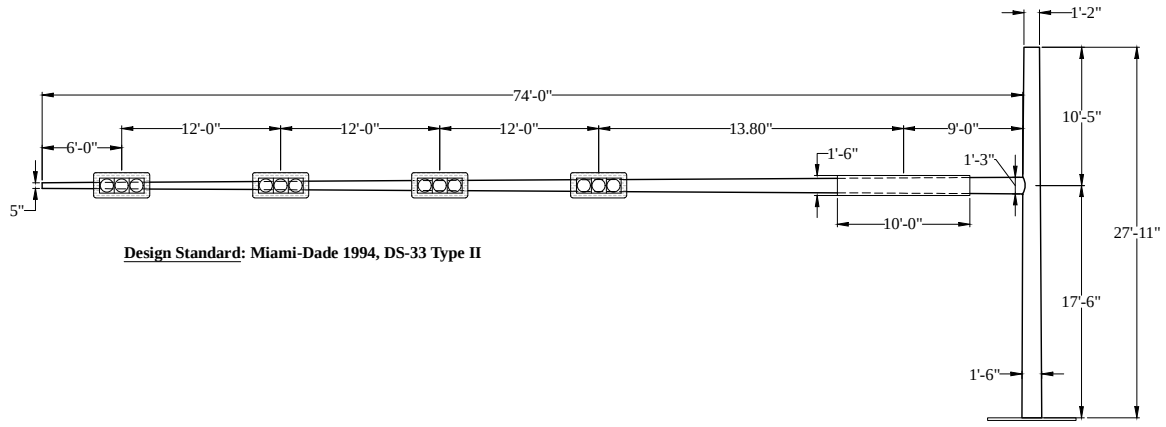

Figure 2-2. Representative FDOT Mast Arm 2

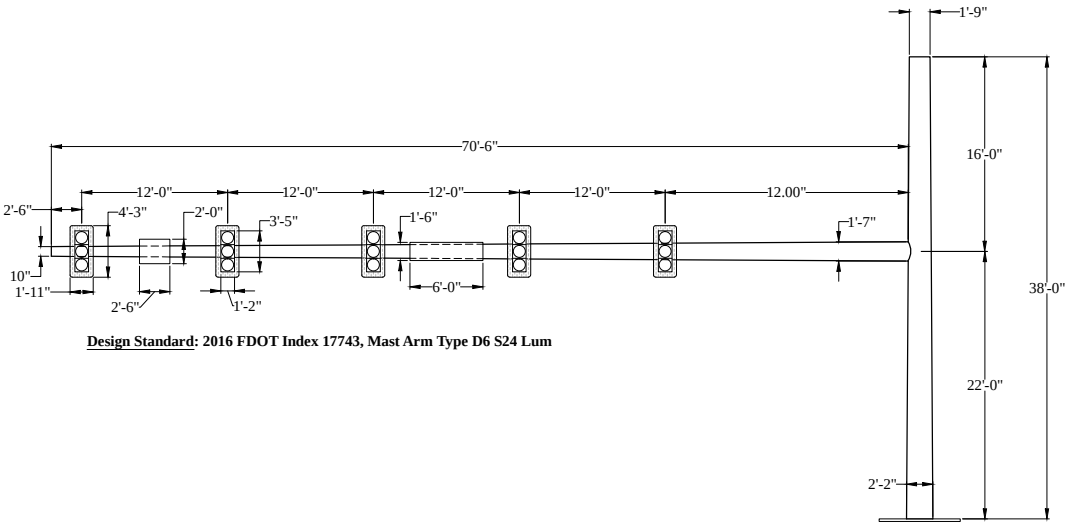

Design Standard: 2016 FDOT Index 17743, Mast Arm Type D6 S24 Lum

Figure 2-3. Representative FDOT Mast Arm 3

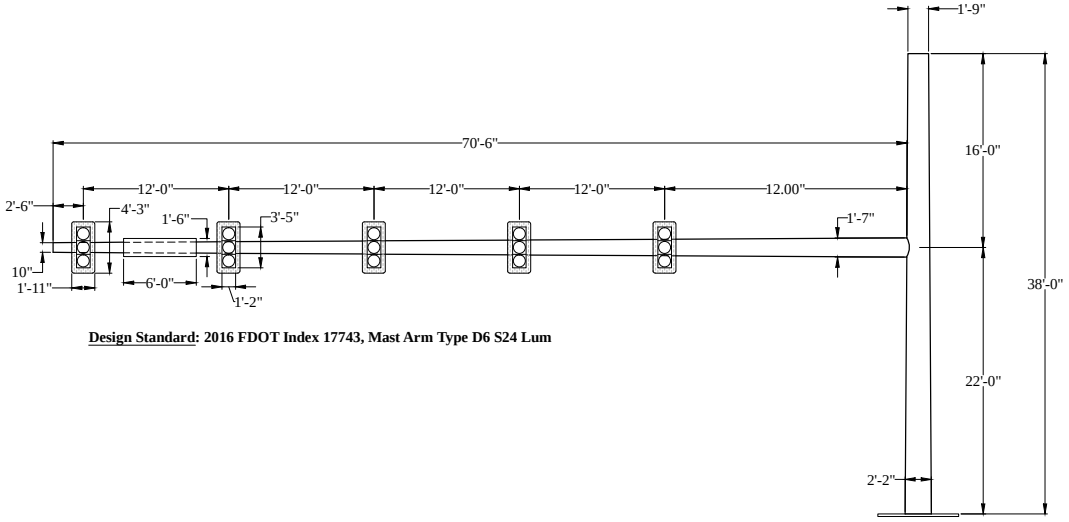

Design Standard: 2016 FDOT Index 17743, Mast Arm Type D6 S24 Lum

Figure 2-4. Representative FDOT Mast Arm 4

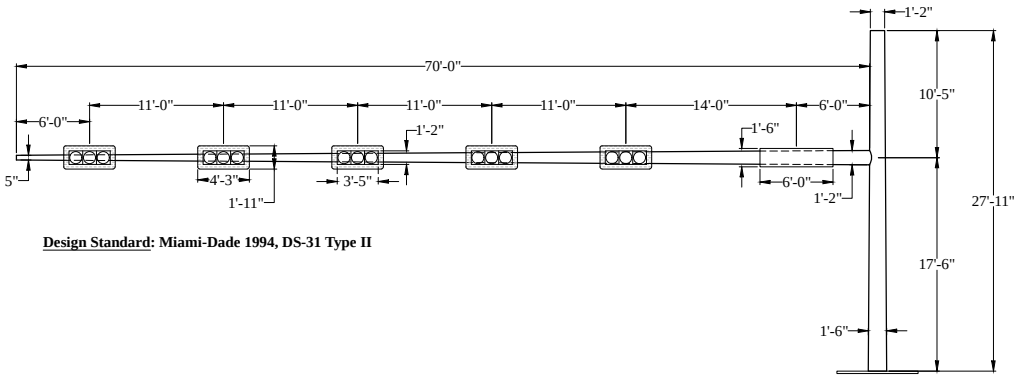

Figure 2-5. Representative FDOT Mast Arm 5

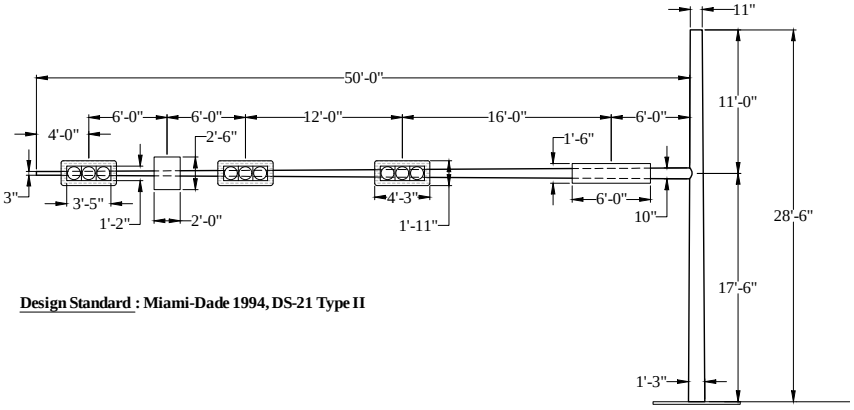

Figure 2-6. Representative FDOT Mast Arm 6

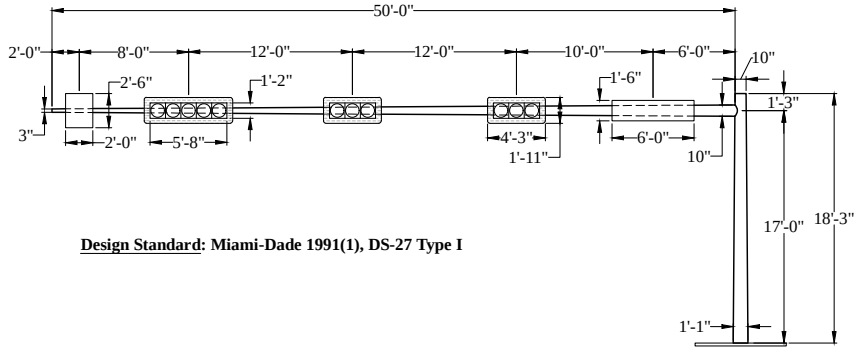

Figure 2-7. Representative FDOT Mast Arm 7

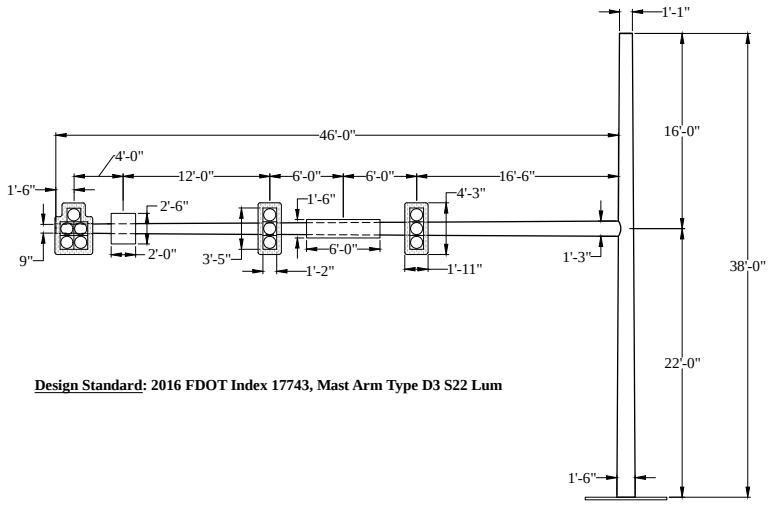

Figure 2-8. Representative FDOT Mast Arm 8

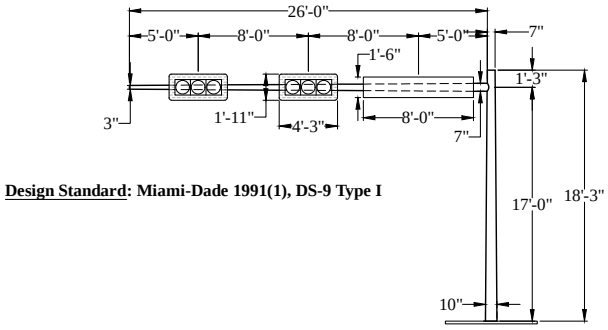

Figure 2-9. Representative FDOT Mast Arm 9

2.3. General Wind Tunnel Testing Methods

Three phases of wind tunnel experiments were conducted: Primary Testing, Supplementary Testing, and Hardware Modification Testing. An in-depth explanation on each testing phase will be given in following sections. This section focuses on the general testing methods that were consistent across each phase of testing.

Each tested model was created using 3D-printed segments that were mounted over a load-carrying steel spine. Figure 2-10 shows the 3D-printed representative Mast Arm 1 reduced-scale model. The 3D-printed segments were created using Visijet M3-X material and a ProJet MJP 3600 Series 3D printer. The steel spine had a square cross-section which ranged from 3/16 to 3/8 inches in thickness (Figure 2-11).

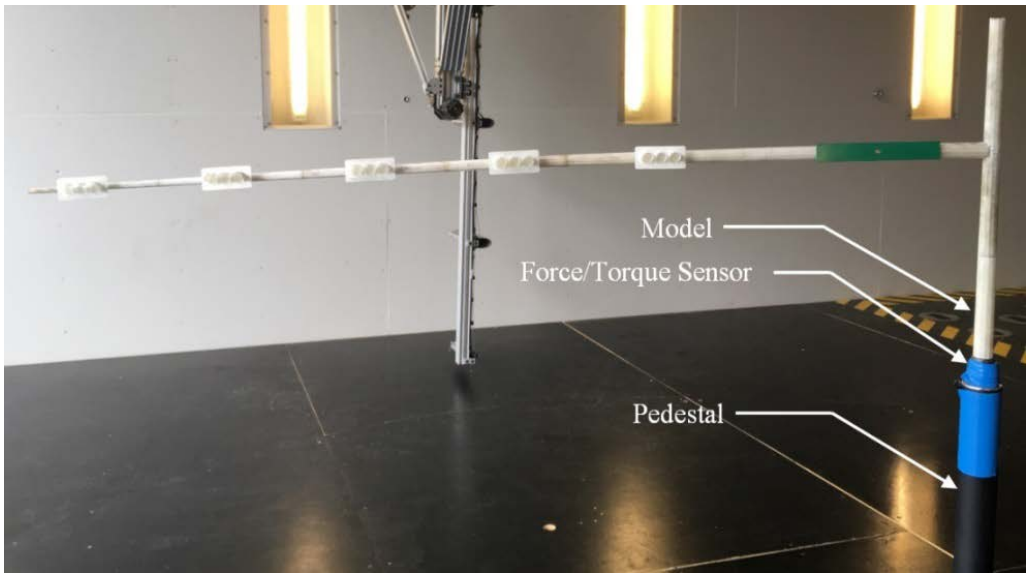

Figure 2-10. Reduced-scale (1:20) model of Mast Arm 1 installed in the wind tunnel

Figure 2-11. Load-carrying square steel spine. (Steel spine on the left is 3/16-inch, and spine on the right is 3/8-inch.)

Wind tunnel testing was conducted at the Boundary Layer Wind Tunnel in the Powell Family Structures and Materials Laboratory at the University of Florida in Gainesville, Florida. The wind tunnel (Figure 2-12) is an open circuit, blowdown (fans are upwind of the test section) wind tunnel with actuated roughness elements and a turntable that is controllable from within the wind tunnel testing control room. In Figure 2-13, a diagram of the test specimen turntable is provided along with the wind tunnel coordinate system. The base of each mast arm model was mounted to a Nano25 IP65 six-axis force/torque sensor from ATI Industrial Automation. The sensor was mounted in such way that its coordinate system matched that of the wind tunnel per Figure 2-13. Outputs from the sensor included forces and moments in all three axes (x-, y-, and z-axes). However, for the purposes of this research, only three base reactions were utilized: along-wind shear (force along the x-axis), over-turning moment (moment about y-axis), and torsion (moment about z-axis). Data was collected at a sampling rate of 100 Hz, and data collection was controlled through LabVIEW software. The force/torque sensor was attached to the top of a 25-inch tall rigid steel vertical pedestal. The base of the pedestal was mounted to the turntable located at the downstream end of the wind tunnel.

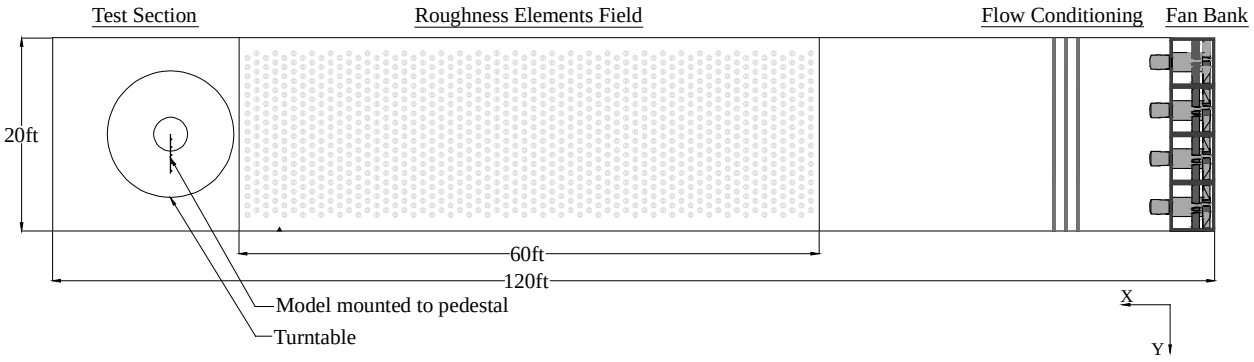

Figure 2-12. Plan view of wind tunnel

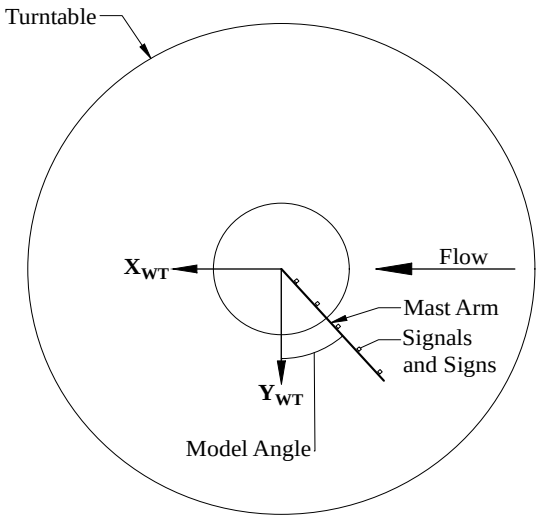

Figure 2-13. Plan view of turntable to which pedestal and test specimens were mounted

Since *mean* drag coefficients for the mast arm structural components were the values of interest in this study, introducing turbulence into the approach flow was not necessary. Turbulence in the approach flow was thus minimized during testing by positioning all the roughness elements in the tunnel flush to the floor, raising the model out of the boundary layer and into the free stream by placing it atop the 25-inch tall steel pipe pedestal, and removing upstream spires (Figure 2-14). Turbulence intensities at the elevated model height (at least 25 inches above the floor) were approximately 4%.

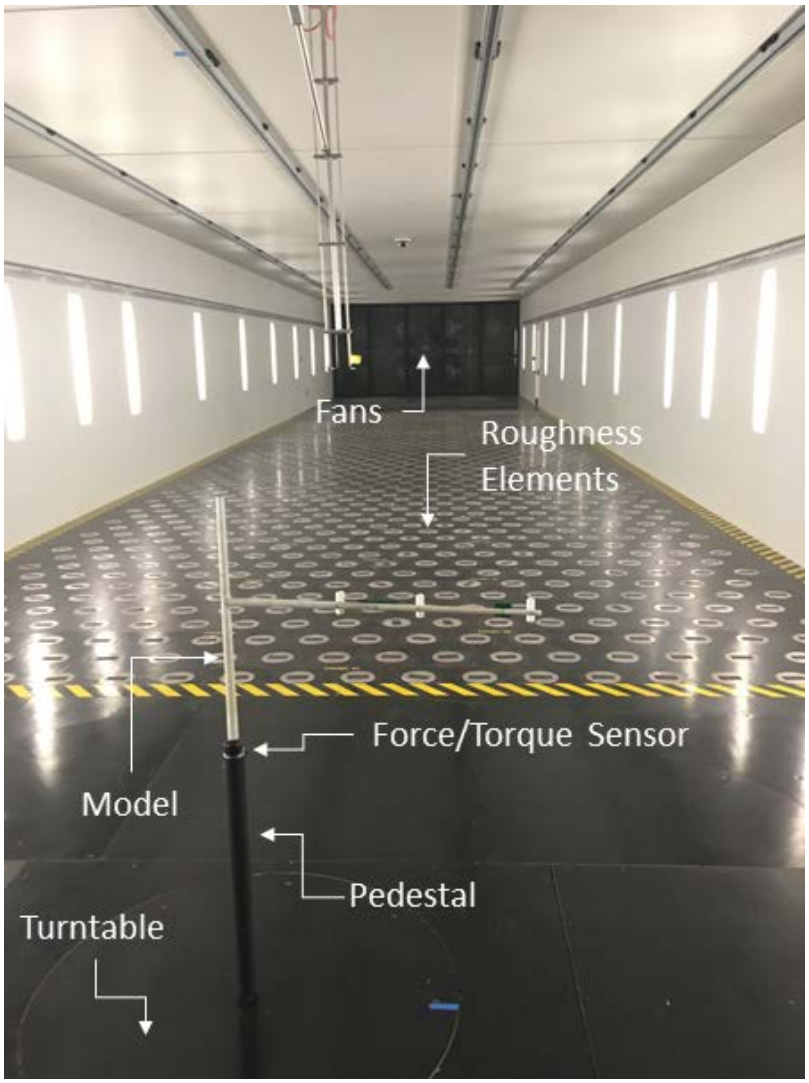

Figure 2-14. Test specimen installed in the wind tunnel

2.4. General Analysis Approach

This section introduces the concept of an incremental drag coefficient (C_{di}), which was used to interpret data from all three phases of wind tunnel testing for the potential presence of aerodynamic shielding.

2.4.1. Incremental Drag Coefficient, C_{di}

As described in Section 2.3, base reaction data (along-wind shear, over-turning moment, and torsion) was collected using a Nano25 IP65 six-axis force/torque load cell. Since this research focused on *static* wind loads on the structure, *mean* base forces and moments were calculated from the collected data. Following this calculation, increases in mean base forces and moments from the addition of attachments were determined for each mast arm by taking the difference between data measured with and without a particular attachment. For instance, to determine the increase in along-wind shear resulting from the addition of signs, base reactions from a 'bare arm' test were subtracted from reactions from an 'arm and signs' test. Analogous calculations involving moments, areas, and eccentricities were used to similarly process measured base moment data. Once the increase in mean base reactions was calculated, the incremental drag coefficient was calculated as:

$$C_{di} = \frac{\Delta R}{A_{att} P_V} \tag{3}$$

where C_{di} is the incremental drag coefficient, ΔR is the incremental increase in mean base reactions, A_{att} is the projected area of attachment, and P_V is mean velocity pressure at arm height, which is calculated using the design wind pressure equation from AASHTO without C_d:

$$P_V = 0.00256 \times K_Z \times K_d \times G \times V^2 \tag{4}$$

For the purpose of calculating the differential C_{di} value, the coefficients in Eq. 4 were set equal to 1.0 (i.e., K_Z = 1.0, K_d = 1.0, and G = 1.0). The incremental drag coefficient, C_{di}, computed in this manner represent the incremental increase of drag force that is generated when signs or signals are attached to a mast arm, and implicitly include the effects of aerodynamic shielding (i.e., reduction of wind load on the portion of the arm that is covered by the attachment). Using the C_{di} concept, total wind loads acting on a mast arm structure would be computed by superimposing drag forces for the bare mast arm (i.e., isolated dodecagonal cylinder) together with incremental drag forces for the attachments (signs, signals). For instance, if a mast arm structure had four signals attached to it and adding an additional signal was desired, the increase in drag force due to the additional signal could be calculated as the product of C_{di}, the area of the signal, and the design velocity pressure. Using C_{di} coefficients in this manner would account for aerodynamic shielding in the calculation process without necessitating changes to the current FDOT design process (which involves superimposing drag forces from individual components).

3. Evaluation of Existing Mast Arm Structures

This section focuses on selected parameters in the FDOT MathCAD program that affect global wind load reactions of mast arm structures. This section also includes an investigation into the selection of drag coefficients based on previous research, as well as results from wind tunnel testing of representative mast arms to study potential effects of aerodynamic shielding.

3.1. Selected Parameters in FDOT Mast Arm Program

A review of the FDOT Mast Arm LRFD v1.0 MathCAD program was conducted, and selected parameters were found to have an influence on computed mast arm capacities. Following are discussions of each of the selected parameters, with potential improvements that could be made to increase the computed mast arm capacity without requiring structural retrofit or replacement.

3.1.1. Height and Exposure Factor

The height and exposure factor (K_Z), which is a function of both height above ground and exposure condition, is a coefficient used to represent height dependent variations of wind speed that occur due to frictional drag caused by terrain roughness. Wind pressures associated with a reference height of 10 meters above ground are modified by K_Z to establish the corresponding wind pressure at the design heights of interest. In the FDOT Mast Arm LRFD v1.0 program, Exposure Category C (as specified in AASHTO LRFD LTS-1) and a single height of 24.4 feet are used to compute K_Z, leading to a value of 0.94. For the representative mast arm structures considered in this study, the vast majority of structural components (arm, signals, and signs) are located at elevations less than 24.4 feet above ground. Using appropriate heights for each major component decreases the K_Z values and thus decreases the corresponding wind pressures. For example, using a mast arm height of 17.5 feet (corresponding to representative Mast Arms 1, 2, 5, 6, 7, and 9) instead of 24.4 feet leads to 7% reductions in K_Z and design wind pressure. While the current approach implemented in the FDOT Mast Arm program is conservative, an increase in computed mast arm capacity would be realized by implementing height-dependent calculations of K_Z.

3.1.2. Mast Arm Connection Plate to Upright Connection

Dead loads and wind loads applied to a mast arm generate forces and moments that must be transferred to the upright pole. To achieve this transfer, a base plate is welded at the end of the mast arm. This plate is bolted to a corresponding base plate located on the pole side of the connection. Forces and moments applied to the pole-side connection plate are transmitted into the upright pole using welded vertical connection plates. In Figure 3-1, the vertical plates are shown in an elevation view of the arm-to-upright connection, as taken from FDOT Index 17745, Sheet 3 (2015). In Figure 3-2, Section F-F from Figure 3-1 is shown in plan-view. In the FDOT Mast Arm program, transmission of load from the pole connection plate to the upright pole is considered to occur *only* through the vertical plates. That is, connection strength contributed by the horizontal plates in the connection is conservatively ignored. If strength contributions from the horizontal plates were instead included in the FDOT Mast Arm program, it is possible that computed structural demands on the vertical side plates might be reduced.

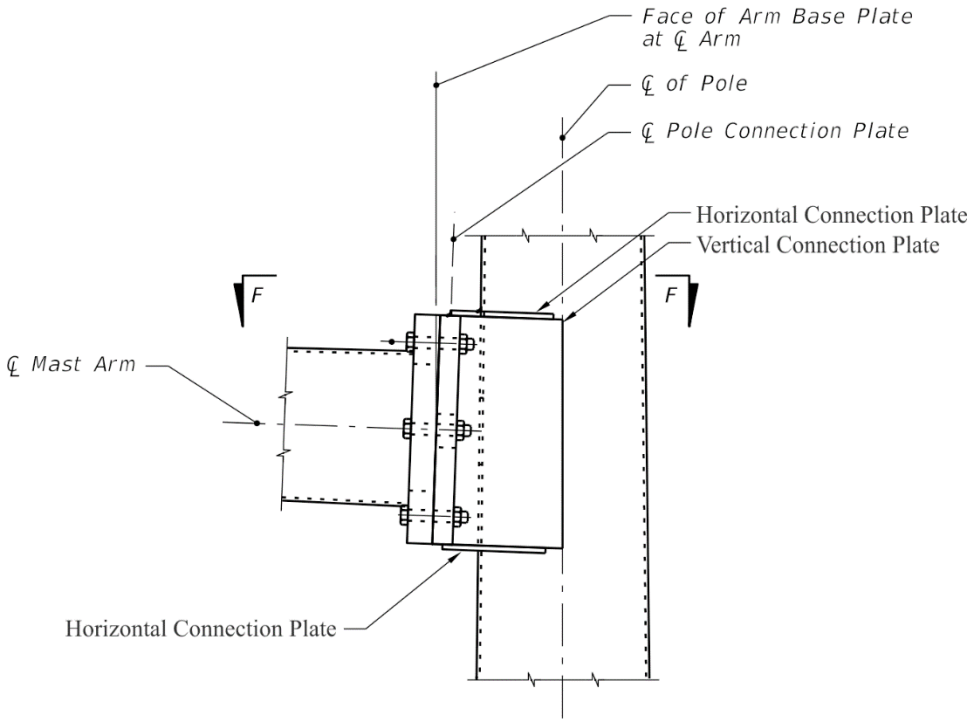

Figure 3-1. Elevation view of mast arm to upright connection

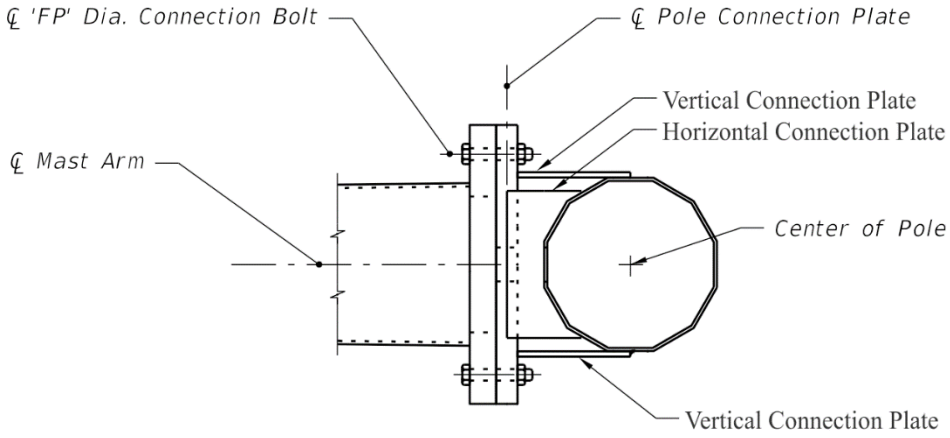

Figure 3-2. Section view of mast arm to upright connection

3.1.3. Gust Effect Factor

The gust effect factor (*G*) specified in AASHTO LRFD LTS-1, is used to modify baseline wind pressure in a manner that approximately accounts for dynamic interactions between a structure and gusts in the wind flow. The gust effect factor is specified in AASHTO LRFD LTS-1 (2015) as *G*=1.14 and is based on the 1.3 gust coefficient used in the AASHTO specifications

(AASHTO LTS-6, 2013). When using the AASHTO LRFD LTS-1 approach, dynamically modified design wind loads are computed as the product of baseline velocity pressure, gust effect factor (G=1.14), mean drag coefficient, and component projected area.

Modal analysis was used in conjunction with provisions in Section 26.9.5 "Gust effects for Flexible or Dynamically Sensitive Buildings or Other Structures" of ASCE/SEI 7-10 Codes and Standards Committee (2010), to compute wind-sensitive gust effect factors for the longest, most-flexible (Mast Arm 1) and shortest, least-flexible (Mast Arm 9) structures considered in this study. Gust effect factor values computed using this approach were found to be significantly larger (G=1.58 for Mast Arm 1, and G=1.33 for Mast Arm 9) compared with the G=1.14 value recommended in AASHTO LRFD LTS-1 (2015).

However, upon further investigation, it was determined that the provisions in ASCE7-10 Section 26.9.5 do not directly address the potentially beneficial effects of aerodynamic damping. Additional components were therefore introduced into the gust effect factor calculation procedure to account for estimated levels of aerodynamic damping. Using modal analysis results, and applying procedures described in Holmes (2007), the "along-wind" aerodynamic damping levels were analytically estimated and found to be considerably larger than structural damping (a finding that is consistent with observations noted in Holmes 1996, Holmes 2007).

The "along-wind" condition was chosen for aerodynamic damping estimation because this loading case is understood to generate the critical design forces for components such as arm-to-pole connection plates. Additionally, the deflected shape caused by the along-wind loading condition is similar in form to the lowest frequency (most wind-sensitive) mode shapes for mast arm structures. After introducing the combined effects of both structural and aerodynamic damping into the ASCE/SEI 7-10 procedures, gust effect factors were analytically re-estimated as G=1.06 for Mast Arm 1, and G=1.03 for the Mast Arm 9. Gust effect factors for mast arms are, however, very sensitive to the combined damping level (aerodynamic plus structural) and can vary significantly for different structural configurations, and for different modes of response. Based on this variability, relevant literature, and calculation results, it is recommended that the AASHTO gust effect factor G=1.14 continue to be used. Consequently, no modifications related to gust effect factor are recommended for implementation in the FDOT Mast Arm Program.

3.1.4. Upright Pole Moment Magnification

Magnification of flexural moment in the upright pole, due to P-Δ effects, is accounted for in the FDOT Mast Arm LRFD v1.0 program using a simplified method outlined in Section 4.8.1 of AASHTO LRFD LTS-1. The method assumes that the upright pole will buckle elastically and specifies a minimum slenderness ratio to ensure elastic behavior. This minimum slenderness requirement is not met by most of the FDOT representative mast arm structures that were considered in this study. The minimum permissible slenderness ratio (kL / r) appears to have been increased from $\sqrt{2}\,\pi\sqrt{E/F_Y}$ in AASHTO LTS-6 to $2\,\pi\sqrt{E/F_Y}$ in AASHTO LRFD LTS-1. Second order (P-Δ) analyses were performed on representative Mast Arms 1 and 9 to quantify moment amplifications using an accurate, geometrically-nonlinear analysis technique (one that considers equilibrium in the deformed configuration of the mast arm). Analyses were performed using the ADINA finite element code and included the combined effects of vertical gravity load (self-weight) and lateral wind load. Moment amplifications quantified from these analyses were:

Mast Arm 1 pole base: M_{wind} amp. = 1.3%; $M_{gravity}$ amp. = 0.3%

Mast Arm 9 pole base: M_{wind} amp. = 0.4%; $M_{gravity}$ amp. < 0.1%

Given the low levels of moment amplification that were computed, no modifications to procedures implemented in the FDOT Mast Arm program are warranted.

3.1.5. Drag Coefficient

For the ultimate strength wind loading condition, the FDOT Mast Arm program uses a drag coefficient of 0.79 for a dodecagonal (12-sided) cylinder, as specified by AASHTO LRFD LTS-1. ESDU 79026 (1980) presents drag coefficients for dodecagonal cylinders that vary depending on corner radius (i.e., corner sharpness), surface roughness, size, approach wind speed, and exposure condition. The AASHTO drag coefficient of 0.79 agrees well with ESDU 79026 (1980) when the latter guidelines are applied to a galvanized mast arm structure designed for a 170-mph 3-second gust wind speed, and with a corner-radius-to-section-diameter ratio of 0.125, i.e. the minimum corner radius permitted by AASHTO LRFD LTS-1. James (1976) demonstrated that as the corner radius of a polygonal tubular section increases, the drag coefficient decreases. Thus, for dodecagonal cylinders with corner radii much greater than 0.125, use of a drag coefficient of 0.79 could be conservative. James (1976) showed that as the number of sides of a polygonal tubular section increases—i.e., the section shape approaches a circle—the drag coefficient correspondingly decreases. Drag coefficients calculated using the methodology presented in ESDU 80025 (1986) confirm that coefficients for round cylinders are smaller than those for polygonal sections of equivalent diameter, as listed in ESDU 79026 (1980) for ultimate wind load cases.

For purposes of computing wind loads on signs, the FDOT Mast Arm program uses a drag coefficient of 1.2, regardless of sign configuration. This value matches that specified by AASHTO LRFD LTS-1 for a sign panel with a length-to-width ratio (i.e., aspect ratio) of 5. However, in AASHTO LRFD LTS-1, Table 3.8.7-1, drag coefficients for signs are also specified as varying with aspect ratio. The FDOT adopted value of 1.2 is conservative for signs with aspect ratios less than 5 (i.e., approaching a square shape) but non-conservative for signs with aspect ratios greater than 5 (i.e., narrow rectangular shapes).

For traffic signals, the FDOT program also uses a drag coefficient of 1.2, as specified in AASHTO LRFD LTS-1, Table 3.8.7-1. The AASHTO recommended value is based on information included in “Wind Forces on Structures” produced by the ASCE Wind Force Committee [ASCE 1961; see also Cook et al. (2007)] for a three-head signal. Use of a signal drag coefficient of 1.2 is based on the assumption that a signal will have a drag coefficient similar to that of a flat plate (e.g., a sign). As will be shown later from results of experimental testing, a drag coefficient of 1.2 for signals is a reasonable approach for design and analysis.

As analyzed by the FDOT Mast Arm program, total wind loads are conservatively computed as the superposition of individual wind loads acting on the mast arm, hardware (signals and signs), and the complete upright pole with no shielding from hardware. Potential aerodynamic shielding effects that may occur between the hardware and arm are currently conservatively neglected. Zdravkovich and Pridden (1977) demonstrated how adjacent cylinders, positioned in-line parallel to wind flow direction, can interfere with the flow condition around the system, thus yielding values of drag coefficients that differ from values quantified for isolated (individual) cylinders. Additionally, prior FDOT-funded research demonstrated that aerodynamic shielding

significantly reduces global wind loads acting on systems of multiple girders positioned in close horizontal proximity (Harper et al. 2016, Consolazio et al. 2014, Consolazio et al. 2013). However, review of relevant literature did not reveal any prior research that has been conducted for the explicit purpose of quantifying the influence that signals and signs have on wind flow around mast arms.

3.2. Primary Testing

Following the review of the FDOT Mast Arm program, experimental wind tunnel testing was conducted to quantify aerodynamic shielding, and assess the suitability of using a drag coefficient of 1.2 for traffic signals and signs. This section focuses on the testing methodology and analysis of results for the first phase of wind tunnel testing.

3.2.1. Wind Tunnel Testing Method

The first phase of experimental testing was conducted using complete reduced-scale 3D printed models of the representative mast arm structures with the purpose of determining whether aerodynamic shielding was present. Maximum geometric scale for the models was limited by the maximum calibrated load sensing range of the multi-axis force/torque sensor (maximum: 25 pound-inch moment) and the maximum expected test loads (self-weight and wind). Worst case loading, from a sensor-capacity perspective, was from representative Mast Arm 1 which had the largest arm (80 feet at full scale), leading to the highest overturning moment. Calculations of spine dead load and expected wind load on Mast Arm 1 showed that a scale model of 1:20 was the largest scale that could be tested without damaging the force/torque sensor. For consistency, the 1:20 scale was used for all mast arm models in this phase of testing. The maximum feasible geometric scale (1:20) was confirmed by experimentally by testing Mast Arm 1 at the anticipated maximum wind load condition (i.e., vertical signals with back plates present and signs attached) and at a wind speed of 10 m/s. Maximum moment (dead and wind) at this test condition was approximately 22 pound-inch, or 88% of the force/torque sensor capacity. The majority (approximately 80%) of load carried by the model was due to self-weight.

Additionally, mast arm angles of 0° (mast arm perpendicular to flow, signals facing approaching flow) and 180° (mast arm perpendicular to flow, signals facing opposite of approach flow) were the primary angles of interest as they caused the highest wind loads. Additional angles ranging from -20° to +20°, and from 160° to 200°, at 5° increments, were also tested to confirm that maximum reactions did, in fact, occur at either 0° or 180°. Combinations of mast arm structures and flow conditions tested in the wind tunnel are summarized in Table 3-1. The last column in Table 3-1 (h/D) refers to the ratio of the height of the attachment to the diameter of the mast arm. Details on the calculation of h/D are given in subsequent sections.

Table 3-1. Test matrix for Primary phase of wind tunnel testing

Test ID	Model Description	Attached Components	h/D
1A	Mast Arm 1	None	-
1D	Mast Arm 1	Signs only	1.20
1E	Mast Arm 1	Signs and horizontal signals w/ back plate	2.42
1F	Mast Arm 1	Signs and horizontal signals w/o back plate	1.45
2A	Mast Arm 2	None	-
2D	Mast Arm 2	Signs only	1.30
2E	Mast Arm 2	Signs and horizontal signals w/ back plate	2.74
2F	Mast Arm 2	Signs and horizontal signals w/o back plate	1.64
3A	Mast Arm 3	None	-
3B	Mast Arm 3	Signs and vertical signals w/ back plate	3.87
3C	Mast Arm 3	Signs and vertical signals w/o back plate	3.10
3D	Mast Arm 3	Signs only	1.68
3E	Mast Arm 3	Signs and horizontal signals w/ back plate	1.74
3F	Mast Arm 3	Signs and horizontal signals w/o back plate	1.04
4A	Mast Arm 4	None	-
4B	Mast Arm 4	Signs and vertical signals w/ back plate	5.02
4C	Mast Arm 4	Signs and vertical signals w/o back plate	4.01
4D	Mast Arm 4	Signs only	2.05
4E	Mast Arm 4	Signs and horizontal signals w/ back plate	2.25
4F	Mast Arm 4	Signs and horizontal signals w/o back plate	1.34
5A	Mast Arm 5	None	-
5D	Mast Arm 5	Signs only	1.36
5E	Mast Arm 5	Signs and horizontal signals w/ back plate	2.72
5F	Mast Arm 5	Signs and horizontal signals w/ back plate	1.62
6A	Mast Arm 6	None	-
6D	Mast Arm 6	Signs only	2.85
6E	Mast Arm 6	Signs and horizontal signals w/ back plate	4.18
6F	Mast Arm 6	Signs and horizontal signals w/o back plate	2.49
7A	Mast Arm 7	None	-
7D	Mast Arm 7	Signs only	2.84
7E	Mast Arm 7	Signs and horizontal signals w/ back plate	3.82
7F	Mast Arm 7	Signs and horizontal signals w/o back plate	2.28
8A	Mast Arm 8	None	-
8B	Mast Arm 8	Signs and vertical signals w/ back plate	4.66
8C	Mast Arm 8	Signs and vertical signals w/o back plate	3.73
8D	Mast Arm 8	Signs only	1.94
8E	Mast Arm 8	Signs and horizontal signals w/ back plate	2.09
8F	Mast Arm 8	Signs and horizontal signals w/o back plate	1.25
9A	Mast Arm 9	None	-
9D	Mast Arm 9	Signs only	2.84
9E	Mast Arm 9	Signs and horizontal signals w/ back plate	4.82

3.2.2. Analysis Approach

Incremental drag coefficients (C_{di}) for various traffic control hardware were calculated and compared to the currently employed drag coefficient of 1.2 specified in AASHTO LRFD LTS-1 to check for potential aerodynamic shielding. Once it was observed that aerodynamic shielding was present, the geometric ratio *h/D*—perpendicular signal dimension (*h*) to arm diameter (*D*)—was used as a means of relating C_{di} to aerodynamic shielding. Figure 3-3 illustrates the height dimension used to determine the *h*/*D* ratio for various component configurations. Figure 3-4 illustrates how a single mast arm diameter was determined by taking a weighted average of signal areas to determine a centroid for the signals. For all models tested in the wind tunnel, the height of all the signal devices were consistent, making the signal area centroid the only value needed to determine a weighted average *h*/*D* geometric ratio.

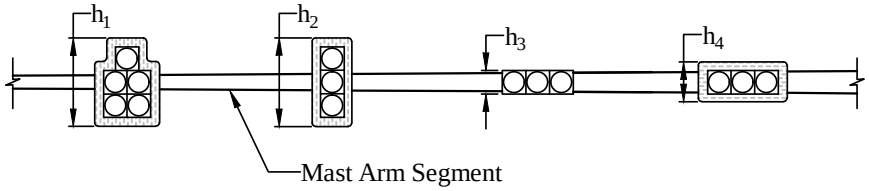

Figure 3-3. Signal height values used to determine geometric ratios, *h*/*D*, for various traffic signals

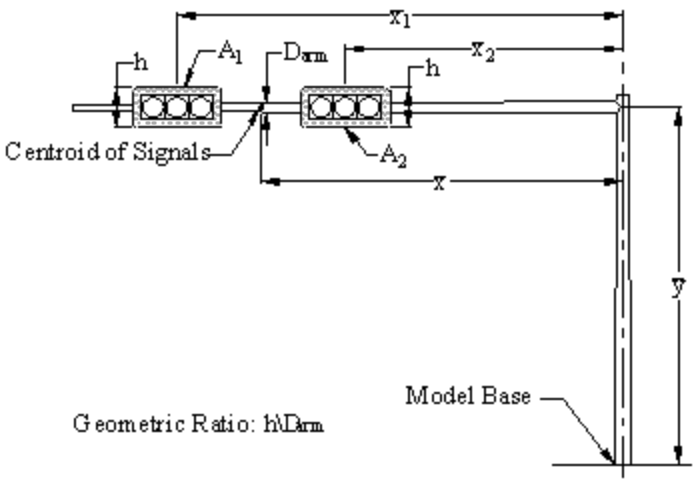

Figure 3-4. Arm diameter used to determine geometric ratio, *h*/*D* (same height signals, oriented parallel to arm)

3.2.3. Results of Primary Testing

Figure 3-5 through Figure 3-9 show C_{di} values for various traffic control hardware as calculated from three different channels on the force/torque sensor: F_x (shear in the along-wind direction), M_y (bending moment about the horizontal axis perpendicular to the along-wind direction), and M_z (moment causing torsion on the upright post cylinder). A C_{di} value of 1.2 would indicate no shielding effect, and that the presence of the sign or signal added a full 1.2 drag factor superimposed on the mast arm (the current conservative design assumption). A C_{di} value less than 1.2 is a quantitative evaluation of partial shielding. A C_{di} value of zero indicates that the addition of the attachment adds no additional load to the system. Thus, a C_{di} value of less than 1.2 represents a potential savings in the current load calculation budget.

It can be observed that the magnitudes of C_{di} in Figure 3-5 through Figure 3-9 are much lower than the drag coefficient of 1.2 specified in AASHTO LRFD LTS-1 for signals and signs. The physical interpretation of this observation is that the segments of the mast arm shielded by the signals are experiencing a wind load lower than the unshielded mast arm segments. Rather than reducing the drag coefficient on the shielded mast arm segments, the reduced load is accounted for by reducing the drag coefficient on the signal providing the shielding as an equivalent proxy. A C_{di} of less than 1.2 does not imply that the signal itself is experiencing wind loads less than a drag coefficient of 1.2. Rather, assigning a C_{di} less than 1.2 to the signal is the mechanism by which the load reduction on the shielded mast arm segment is implemented.

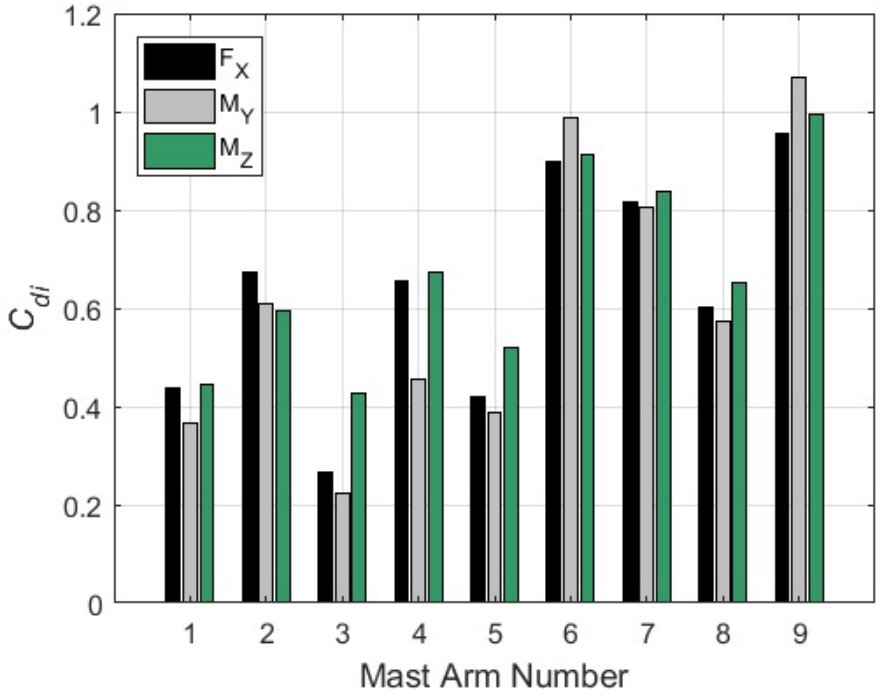

Figure 3-5. C_{di} data for signal with back plate oriented parallel to arm (horizontal)

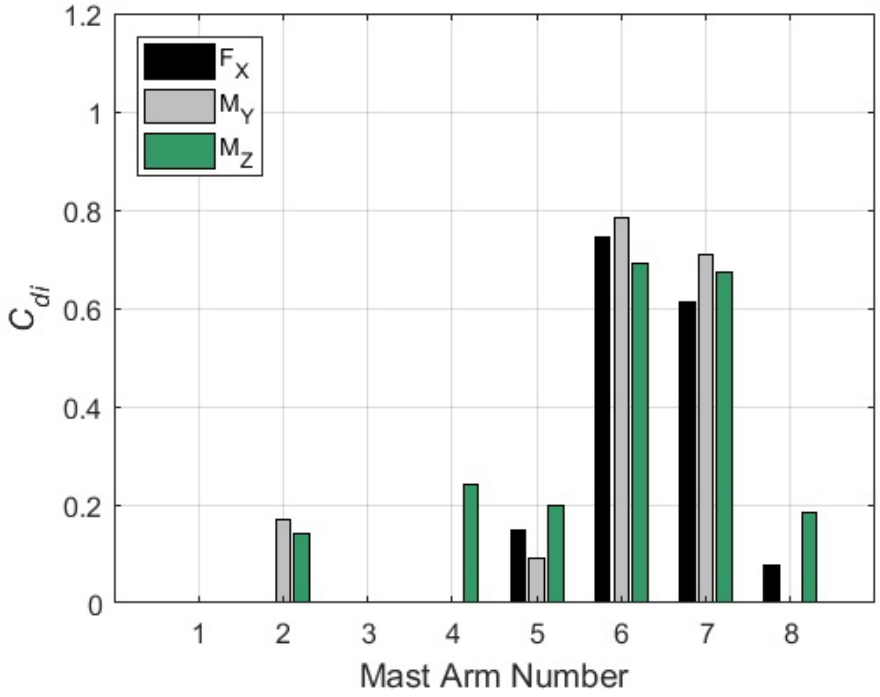

Figure 3-6. C_{di} data for signal without back plate oriented parallel to arm (horizontal)

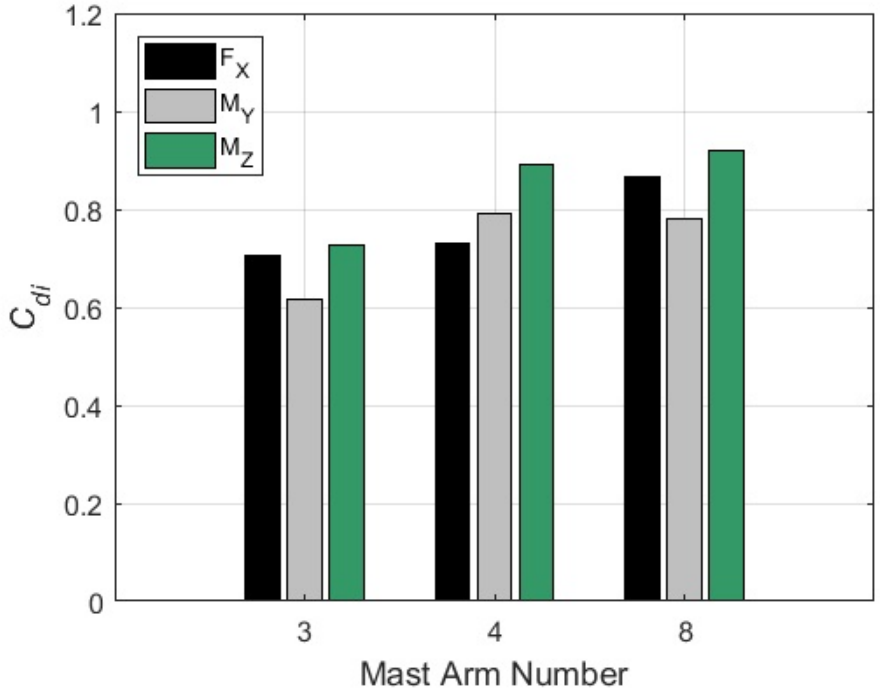

Figure 3-7. C_{di} data for signal with back plate oriented perpendicular to arm (vertical)

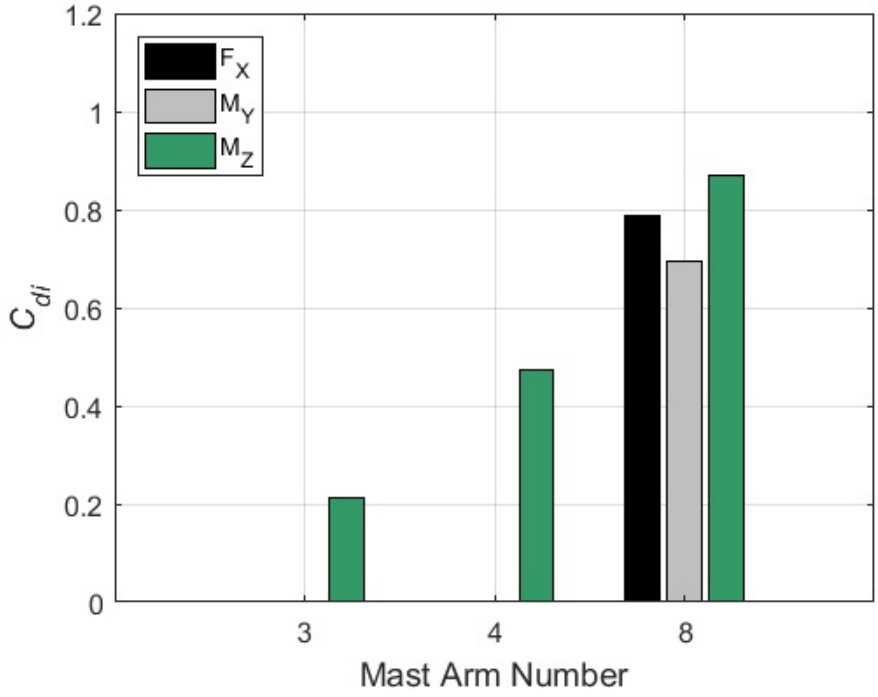

Figure 3-8. C_{di} data for signal without back plate oriented perpendicular to arm (vertical)

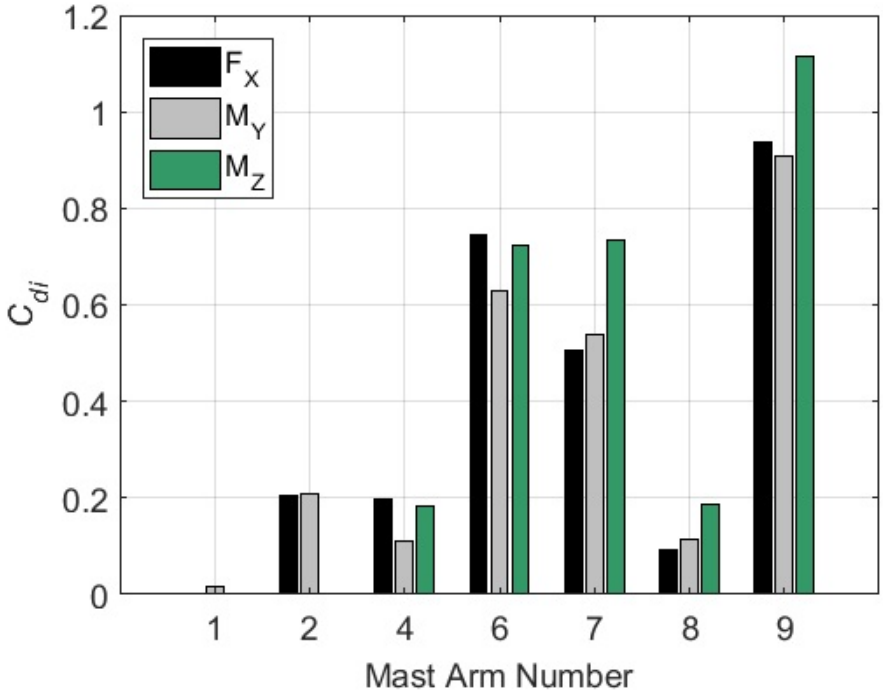

Figure 3-9. C_{di} data for sign configuration

Some sensor data channels produced C_{di} values that were nearly zero or moderately negative. Such cases were observed for signals without back plates (both horizontal and vertical orientations) mounted on larger diameter mast arms. For such cases, the essentially negligible increase in load produced by attachment of signals was below the force level that could be accurately measured using the force/torque sensor employed. However, when overall load on the structure was increased (e.g., by addition of back plates), agreement between the various channels on the force/torque sensor improved substantially. Consequently, C_{di} values were set to zero for cases in which negligible incremental drag forces were observed.

Figure 3-10 presents C_{di} values for various traffic signal configurations based on averaging values determined from non-zero force/torque sensor channels (values in previous figures). The C_{di} data are plotted against the ratio of hardware height to pole diameter (h/D). Incremental drag coefficients were generally observed to increase with corresponding increases in h/D. For signs (versus signals), Figure 3-11 shows a similar trend, that C_{di} coefficients generally increased as the ratio of sign height to pole diameter increased.

The interpretation of these trends is that the overestimation of wind loads using the current approach of superposition of full wind pressure (ignoring shielding effects) becomes less significant as the relative size of the sign or signal—in relation to the pole being shielded—gets larger. Conversely, the current approach of including the full wind load of the both the mast arm and sign or signal becomes more conservative in cases where the height of the sign or signal is very similar to the diameter of the mast arm being shielded.

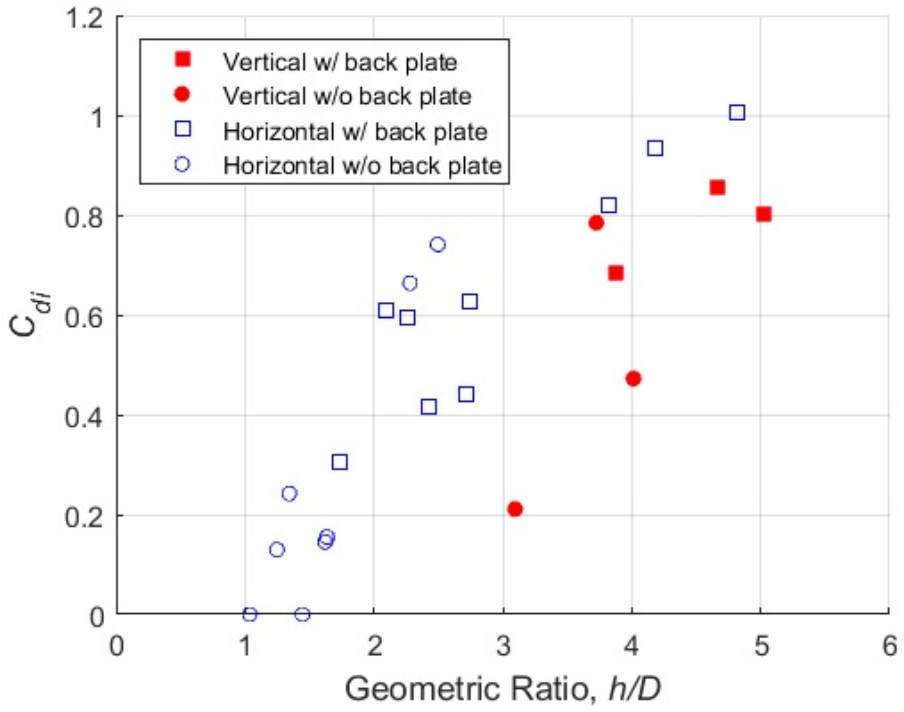

Figure 3-10. Signal incremental drag coefficients (C_{di}) versus geometric ratio (h/D)

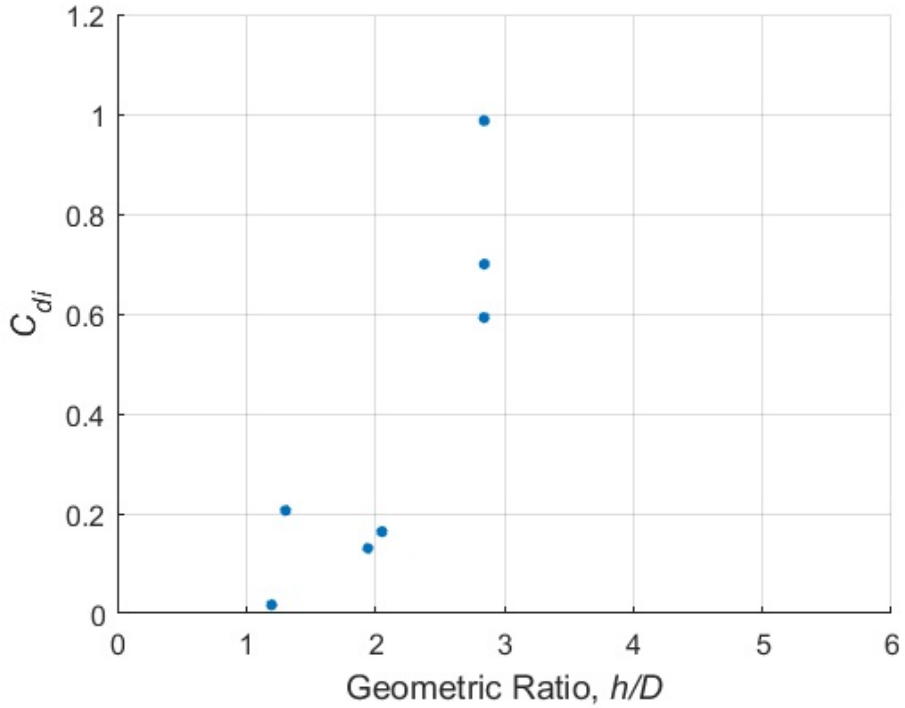

Figure 3-11. Sign incremental drag coefficients (C_{di}) versus geometric ratio (h/D)

3.3. Supplementary Testing

Results presented for Primary Testing were determined from global loads for complete mast arm assemblies. Greater uncertainty should be expected when calculating an individual component C_{di} from a full mast arm assembly, as opposed to obtaining such values from tests of individual traffic signals, individual signs, or individual pole sections. Additionally, equipment constraints (capacity of the force/torque sensor and wind tunnel test section dimensions) associated with testing led to a maximum geometric scale of 1:20 for the mast arm assemblies. Consequently, supplementary component-level testing was conducted to investigate the sensitivity of previously presented C_{di} results to multiple test parameters.

3.3.1. Wind Tunnel Testing Method

Tests were conducted on a single traffic signal or sign mounted on a single vertical pole. This simpler configuration permitted a larger model geometric scale of 1:8 and enabled testing of a wider range of height to arm diameter ratios with varying hardware offset distances. Two different (dodecagonal cylinder) pole diameters were considered. In addition to the two pole diameters, single traffic signals and signs mounted on a narrow steel spine were tested to determine 'isolated' drag coefficients (the drag coefficient of the signal or sign in isolation). The test matrix for the supplementary testing is shown in Table 3-2. All dimensions in the table are at model scale.

Table 3-2. Test matrix for Supplementary phase of wind tunnel testing

Test ID	Model Description	Attached Components	h/D
SPINE	Bare Steel Spine	None	-
CYL1	0.375” Dodecagon Cylinder	None	-
CYL2	2.125” Dodecagon Cylinder	None	-
SPINE_B	Bare Steel Spine	Parallel signal w/ back plate	-
CYL1_B	0.375” Dodecagon Cylinder	Parallel signal w/ back plate	7.70
CYL2_B	2.125” Dodecagon Cylinder	Parallel signal w/ back plate	1.34
SPINE_C	Bare Steel Spine	Parallel signal w/o back plate	-
CYL1_C	0.375” Dodecagon Cylinder	Parallel signal w/o back plate	4.56
CYL2_C	2.125” Dodecagon Cylinder	Parallel signal w/o back plate	0.80
SPINE_E	Bare Steel Spine	Perpendicular signal w/ back plate	-
CYL1_E	0.375” Dodecagon Cylinder	Perpendicular signal w/ back plate	17.2
CYL2_E	2.125” Dodecagon Cylinder	Perpendicular signal w/ back plate	2.39
SPINE_F	Bare Steel Spine	Perpendicular signal w/o back plate	-
CYL1_F	0.375” Dodecagon Cylinder	Perpendicular signal w/o back plate	13.7
CYL2_F	2.125” Dodecagon Cylinder	Perpendicular signal w/o back plate	2.39
SPINE_S1a	Bare Steel Spine	1.5” x 1.2” sign	-
CYL1_S1a	0.375” Dodecagon Cylinder	1.5” x 1.2” sign	3.24
CYL2_S1a	2.125” Dodecagon Cylinder	1.5” x 1.2” sign	0.57
SPINE_S1b	Bare Steel Spine	1.2” x 1.5” sign	-
CYL1_S1b	0.375” Dodecagon Cylinder	1.2” x 1.5” sign	4.05
CYL2_S1b	2.125” Dodecagon Cylinder	1.2” x 1.5” sign	0.71
SPINE_S2a	Bare Steel Spine	4” x 2” sign	-
CYL1_S2a	0.375” Dodecagon Cylinder	4” x 2” sign	5.41
CYL2_S2a	2.125” Dodecagon Cylinder	4” x 2” sign	0.94
SPINE_S2b	Bare Steel Spine	2” x 4” sign	-
CYL1_S2b	0.375” Dodecagon Cylinder	2” x 4” sign	10.8
CYL2_S2b	2.125” Dodecagon Cylinder	2” x 4” sign	1.89

Test ID Key		
Support_Attachment		
	Support	
	SPINE	Steel Spine
	CYL1	Smaller Dodecagon Cylinder
	CYL2	Larger Dodecagon Cylinder
	Attachment	
	B to K	Various signals as described in column 3 above
	S1	Smaller Sign
	S2	Larger Sign
	a	Sign Parallel w/ Support
	b	Sign Perpendicular to Support

Each configuration in Table 3-2 was tested at nominal wind speeds of 5, 10, and 15 m/s. Each signal attachment configuration was tested with horizontal signal offset distances of 1.25 inch, 1.75 inch, and 2.25 inch (measured from front face of signal housing to the closest point on the mast arm [Figure 3-12]); all signs were mounted flush to the supports (Figure 3-14). Model orientations of 0° (signal or sign perpendicular and facing approaching flow) and 180° (signal or sign perpendicular and facing opposite the approach flow) were tested. The different wind speeds, hardware offsets, and model orientations resulted in 18 different data collection trials for each signal Test ID. Figure 3-13 shows a typical supplementary phase wind tunnel test.

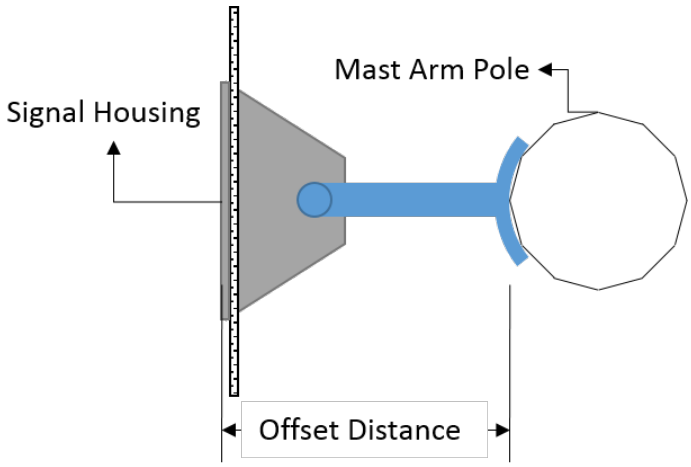

Figure 3-12. Drawing illustrating offset distance

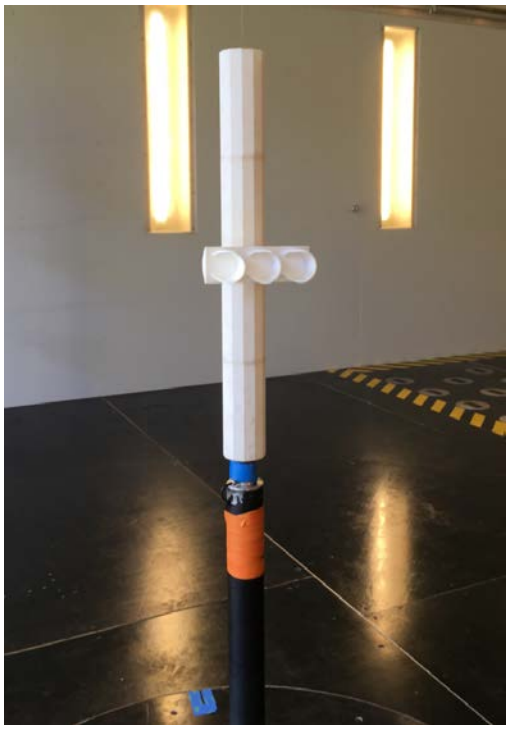

Figure 3-13. Wind tunnel test CYL2_F – Cylinder 2, 1:8 scale, perpendicular signal without back plate mounted to dodecagon cylinder

Figure 3-14. Model signal mounted flush onto Cylinder 2

3.3.2. Supplementary Testing Results

C_{di} values were calculated for each tested configuration as described previously. Figure 3-15 and Figure 3-16 present C_{di} values for the configurations tested (signals and signs, respectively) as functions of geometric ratio (h/D). Results from Primary Testing (smaller scale, full assembly) are also included in these figures for comparison. Figure 3-17 superimposes data from Figure 3-15 and Figure 3-16 to consolidate all of the tested configurations from both primary and supplementary testing. In each of these figures, multiple data points with the same icon are observed at various h/D values. These data points represent C_{di} values calculated for the different wind speeds, offsets, and measured reactions (moment and shear) at each h/D value. During data analysis, it was determined that for tests at wind speeds of 5 m/s, the incremental loads caused by adding a signal or sign to the pole fell below the force level that could be accurately measured using the multi-axis load cell sensor employed, thus all 5 m/s data were omitted from the analysis. In addition to omitting the 5 m/s data, test IDs CYL1_S1a and CYL1_S1b were likewise excluded from Figure 3-16 due to unreliably small incremental loads. In Figure 3-15 through Figure 3-17, bilinear functional forms, each with a plateau value of 1.2, were fit to the data using square error minimization. Equations for each fit are given in their respective figures.

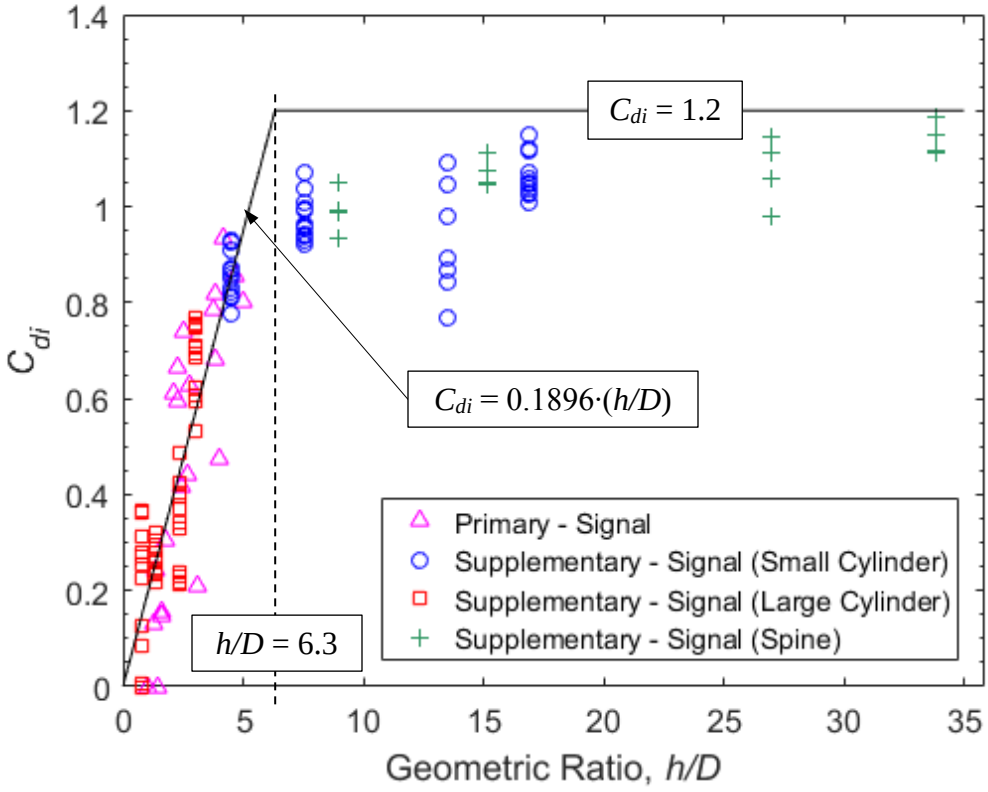

Figure 3-15. Signal incremental drag coefficients versus geometric ratio (h/D)—primary and supplementary testing

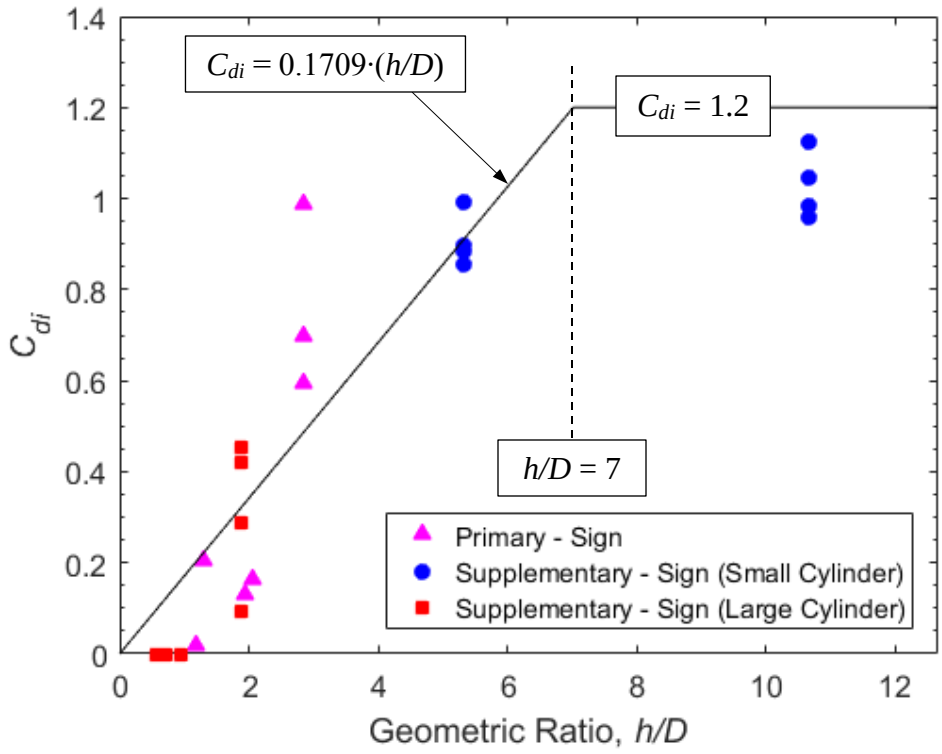

Figure 3-16. Sign incremental drag coefficients versus geometric ratio (*h*/*D*)—primary and supplementary testing

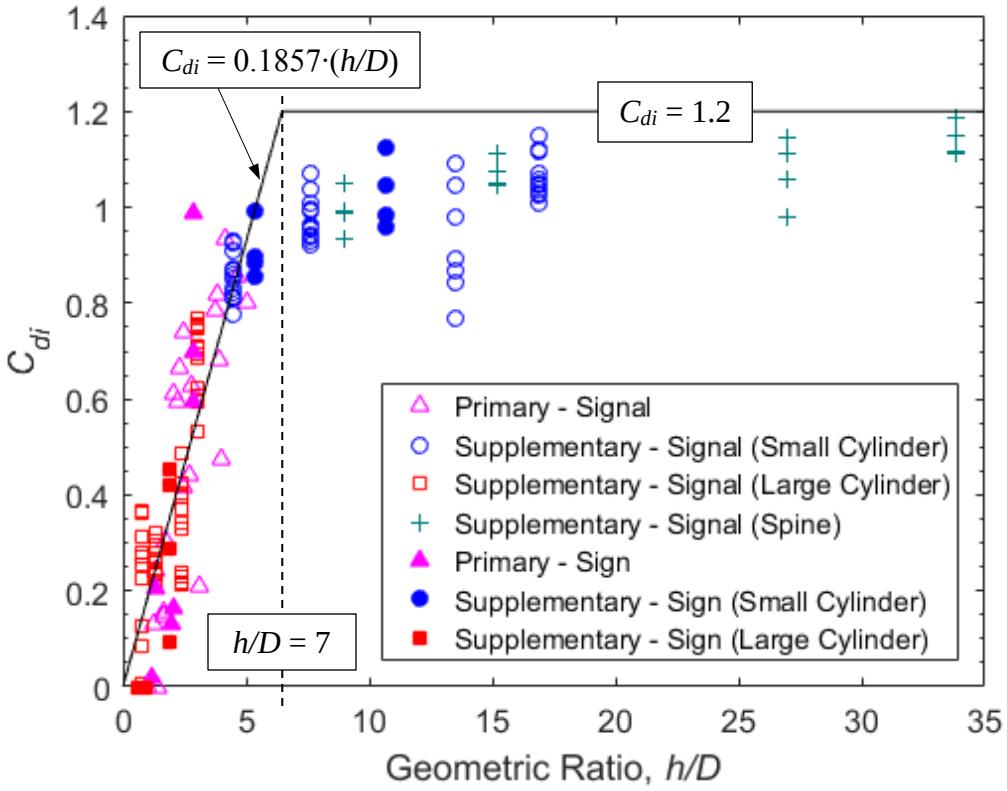

Figure 3-17. Signal and sign incremental drag coefficients versus geometric ratio (*h/D*)—primary and supplementary testing

In corresponding fashion to the Primary Testing results, a C_{di} value less than or equal to zero indicated that the addition of the attachment added no additional load to the system, and thus were set to zero. These cases were most frequently observed with signs (Figure 3-16) that had a geometric ratio of *h/D* less than one. Furthermore, a trend can be observed—more prominently in Figure 3-15 and Figure 3-17—that as *h/D* increased, C_{di} increased, converging towards a plateau of 1.2 (i.e. the ratio of attachment height to pole diameter was such that shielding effects became negligible). The observed trend reinforces the concept that there is potential savings in the current load calculation budget in the cases where *h/D* falls within the low *h/D* cloud before the plateau, and that additional hardware is unlikely to add significant load when the height (*h*) of such hardware is equal to or less than the diameter of the pole (*D*) at the attachment location. No discernable pattern, or stratification, was observed in the data due to differences in signal offsets (i.e. smaller offsets did not consistently yield smaller or larger C_{di} values). Lastly, the results in Figure 3-17 combine multiple tests, two different scales, and two different wind speeds, and therefore a span range of Reynolds numbers. The incremental drag coefficient approach (the quantification of incremental drag coefficients based on the difference in loading with and without attachments) was developed and applied in this study to mitigate Reynolds number mismatch issues between scale model and full scale. No discernable pattern or stratification related to Reynolds number was identified in Figure 3-17. This supports the hypothesis that incremental drag coefficients identified at reduced-scale model (1:20, 1:8) Reynolds numbers are suitable for extrapolation to full scale.

Figure 3-18 and Figure 3-19 present the same data as Figure 3-17, however the fit through the data differs. Figure 3-18 uses a bilinear functional form fit with the slope of the fit through the low *h/D* cloud adjusted so that it envelopes 95% of the data points. Figure 3-19 uses a hyperbolic fit with coefficients adjusted so that 95% of the data points are below the curve. The hyperbolic fit is given by:

$$C_{di} = \frac{1.44\left(h/D\right)^2}{1.2\left(h/D\right)^2 + 1.44\left(h/D\right)} \tag{5}$$

As can be observed from the figures, the hyperbolic fit offers a better fit of the data, more accurately modeling the transition phase between the low *h/D* cloud and plateau.

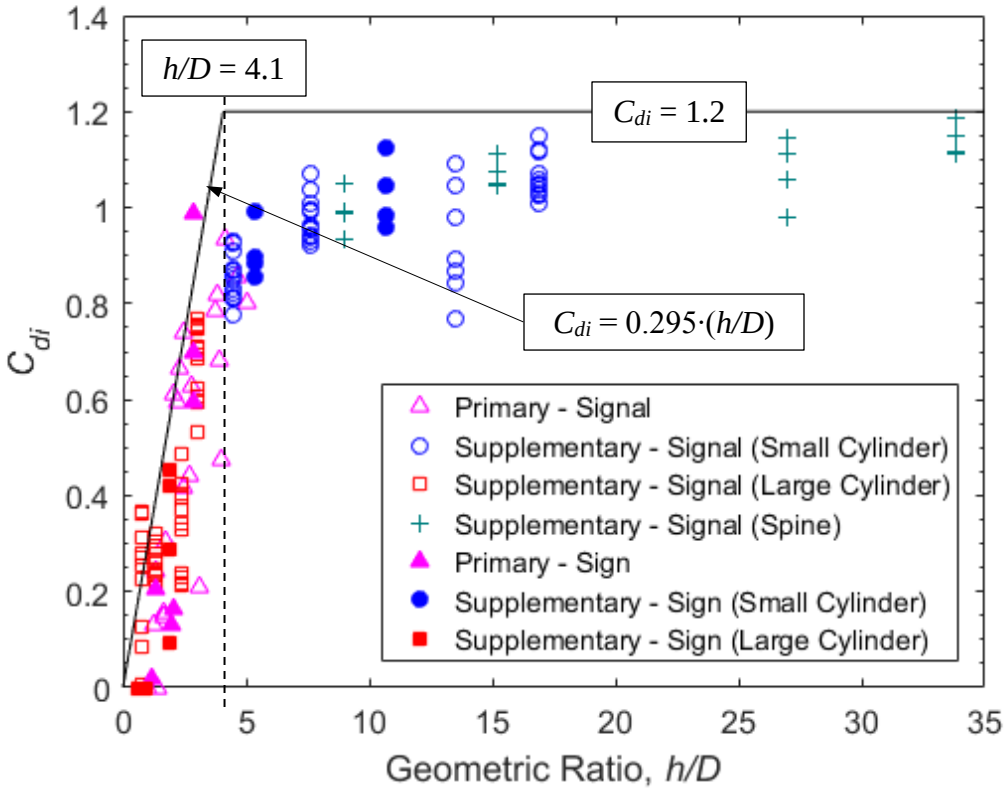

Figure 3-18. Signal and sign incremental drag coefficients versus geometric ratio (*h*/*D*) with 95% bilinear envelope

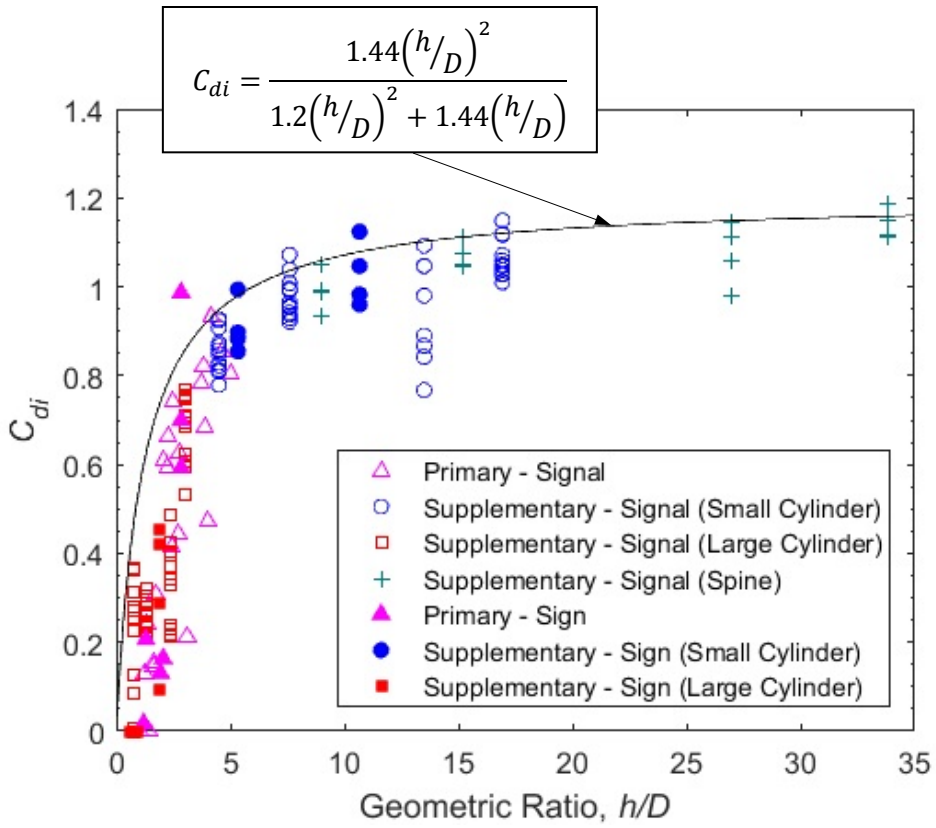

Figure 3-19. Signal and sign incremental drag coefficients versus geometric ratio (*h*/*D*) with 95% hyperbolic envelope

4. Proposed Modifications to Analytical Procedures

Based on reviewed parameters in the FDOT Mast Arm LRFD v1.0 program, it was determined that selected parameters could have an impact on important structural demands (e.g., global wind load reactions). In this section, proposed modifications to selected parameters were implemented into the FDOT Mast Arm program (henceforth referred to as "parameter-modified program"). Reactions (shear, over-turning moment, and torsion) at the base of the mast arm structure due to ultimate wind loads were then compared to the reactions determined using the FDOT unmodified Mast Arm LRFD v1.0 program (henceforth referred to as "current FDOT Mast Arm program"). The key parameters that could be modified and significantly influence design wind loads were identified as the drag coefficients (C_d) of signs and signals and the height and exposure factor (K_Z). The influence of implementing modified C_d and K_Z values is investigated in the following sections.

4.1. Proposed Analytical Modifications to Selected Parameters

4.1.1. Height and Exposure Factor

In the current FDOT Mast Arm program, calculation of the exposure factor is performed using a single height of 24.4 feet for every mast arm, independent of the actual height of the arm. However, the vast majority of structural components (e.g., signals and signs) on representative mast arms are located below an elevation of 24.4 feet. Thus, the proposed modification to this parameter is that the calculation be performed using the actual arm height, yielding a K_Z value that is specific to the mast arm being designed and/or analyzed. Accounting for true component heights will yield lower values of K_Z and lower wind pressures.

4.1.2. Drag Coefficient

In the current FDOT Mast Arm program, a default drag coefficient of 1.2 is used for traffic signals and signs, as specified in AASHTO LRFD LTS-1, Table 3.8.7-1. Wind pressure is also calculated for the full bare mast arm and superimposed with the attachment loading. This conservative approach does not account for the attachments partially shielding portions of the mast arm from wind loading, and results in the same loading for both horizontal and vertical signal configurations.

Rather than reducing the wind loading on the shielded portions of the mast arm, the proposed modification is to replace the drag coefficient constant of 1.2 currently assigned to the attachments with an experimentally determined incremental drag coefficient (C_{di}), which is bounded by [0, 1.2], and which implicitly contains the influence of shielding. Wind load is calculated and applied to the full bare mast arm as in the current method. In this approach, shielding is represented by applying a reduced wind load on each attachment, which is quantified by the C_{di} that replaces the constant 1.2. The appropriate C_{di} for a given attachment is dependent upon the ratio (h/D) of the height (h) of the attachment (perpendicular to mast arm) to the diameter of the mast arm where attachment is located (D). This relationship between C_{di} and h/D is modeled by a hyperbolic fit that envelopes 95% of the experimental data (Eq. 5). In this manner, the difference in shielding (and resultant loading) of the mast arm between vertical and horizontal orientations is accounted for.

In the proposed hyperbolic fit, C_{di} is bounded by the range [0, 1.2]. In terms of implementation, however, FDOT will employ a modified hyperbolic fit which is bounded instead

by the range [0.8, 1.2]. The FDOT bounded values were established based on practical minimum and maximum values of *h/D*, respectively, as per attachment dimensions in their inventory. The FDOT modified hyperbolic fit is presented in Appendix A.

4.2. Implementation of Proposed Analytical Modifications

4.2.1. Height and Exposure Factor

To implement the proposed modification to the K_Z value at the arm height, a minor change was implemented in the current FDOT Mast Arm program. The change was in the definition of the variable "$height_{arm}$" from 24.4 feet (Figure 4-1) to the height of arm-to-pole connection, "$Y_{arm.conn}$" (Figure 4-2). This change will allow the K_Z value for the arm to be calculated based on the actual mast arm height. No change was implemented for determining K_Z for the upright pole, as the current procedure was determined to be appropriate.

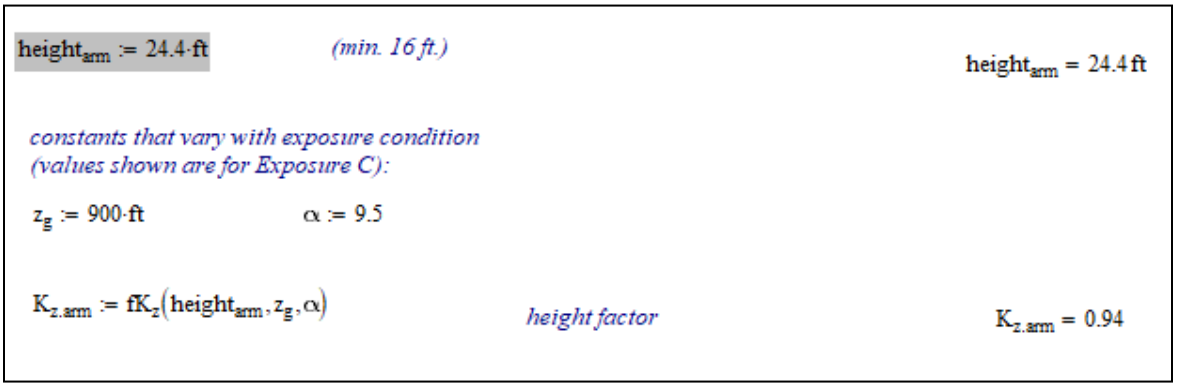

Figure 4-1. Sample of current FDOT Mast Arm program illustrating static definition of "*height*$_{arm}$" (representative Mast Arm 1 used as example)

Figure 4-2. Sample of modified FDOT Mast Arm program illustrating dynamic definition of "*height*$_{arm}$" (representative Mast Arm 1 used as example)

4.2.2. Drag Coefficient

The incremental drag coefficient (C_{di}) is assigned individually for each attachment (signal or sign) as a function of the height to mast arm diameter ratio (*h/D*) using Eq. 5. This approach accounts for aerodynamic shielding specific to the dimensions of the given attachment as well as the attachment orientation (horizontal or vertical). To account for signal orientation, the current FDOT Mast Arm program was adapted to include "Orientation" (Figure 4-3). To determine *h/D* ratios for signs, it was necessary to modify the current FDOT Mast Arm program and input file to replace the input "$Area_{panel.arm1}$" with the dimensions of the sign (height and width), and then calculate the area within the program (Figure 4-3). Full integration of the proposed modification, making use of C_{di} determined using *h/D*, will require FDOT to modify their input file accordingly.

The current FDOT Mast Arm program was adapted to include C_{di} calculations for signals and signs. C_{di} calculations for signals are performed in the "Signal DL and WL Moments and Shears" section, while C_{di} calculations for signs are performed in the "Sign Panel DL and WL Moments and Shears". The geometric ratio (*h/D*) for each attachment on the mast arm is first determined. This calculation is performed using already-defined variables within the program (Figure 4-4 and Figure 4-5). The C_{di} for each attachment is then calculated using Eq. 5 with the geometric ratio *h/D* as the independent variable (Figure 4-6).

Arm 1 Analysis DataFile = "Candidate 1 - BP - Modded.dat" WindSpeed = 150·mph

Arm 1 Loads

$SignalData_{arm1} =$

"SignalNumber"	"DistanceToSignal(ft)"	"NumberofSignalHeads"	"BackPlate"	"Orientation"
1	27	3	"no"	"horizontal"
2	39	3	"no"	"horizontal"
3	51	3	"no"	"horizontal"
4	63	3	"no"	"horizontal"
5	75	3	"no"	"horizontal"
6	0	0	"no"	"horizontal"
7	0	0	"no"	"horizontal"
8	0	0	"no"	"horizontal"
9	0	0	"no"	"horizontal"
10	0	0	"no"	"horizontal"

$SignData_{arm1} =$

"PanelNumber"	"DistanceToPanelCentroid(ft)"	"PanelWidth(ft)"	"PanelHeight(ft)"
1	9	10	1.5
2	0	0	0
3	0	0	0
4	0	0	0
5	0	0	0

Figure 4-3. Section of modified FDOT Mast Arm program to account for signal orientation (top) and dimensions of sign (bottom)

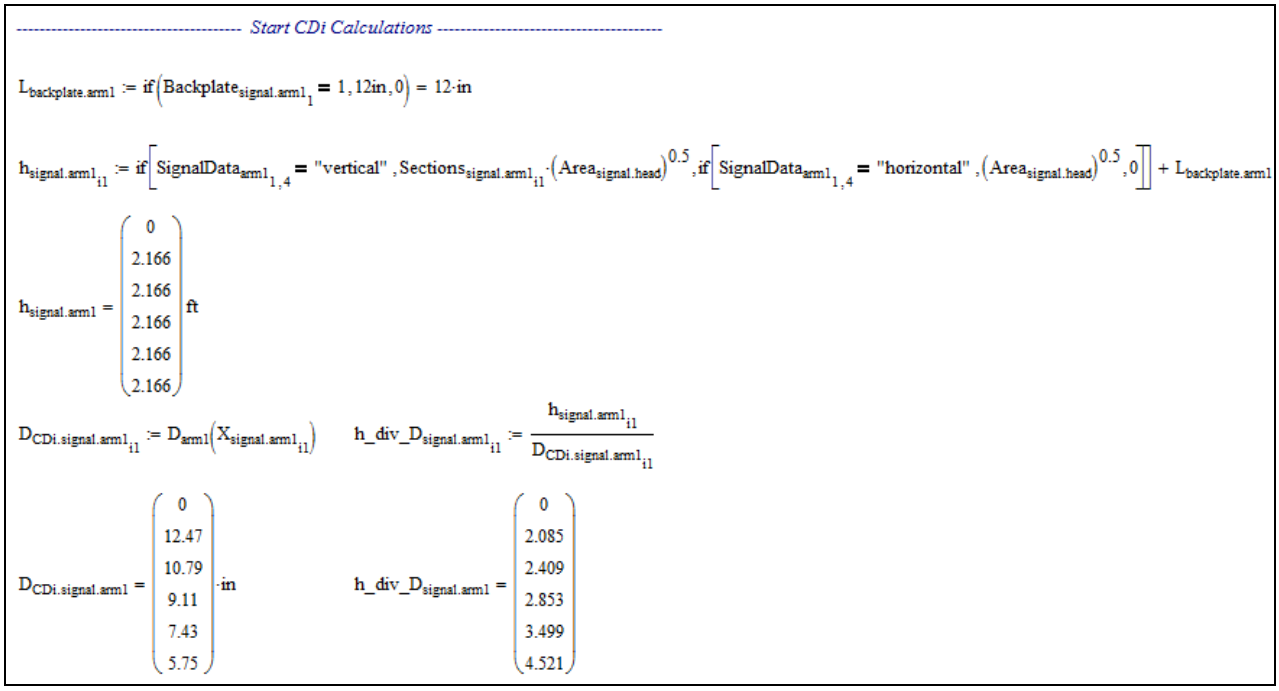

Figure 4-4. Individual geometric ratio (*h/D*) determination for signals

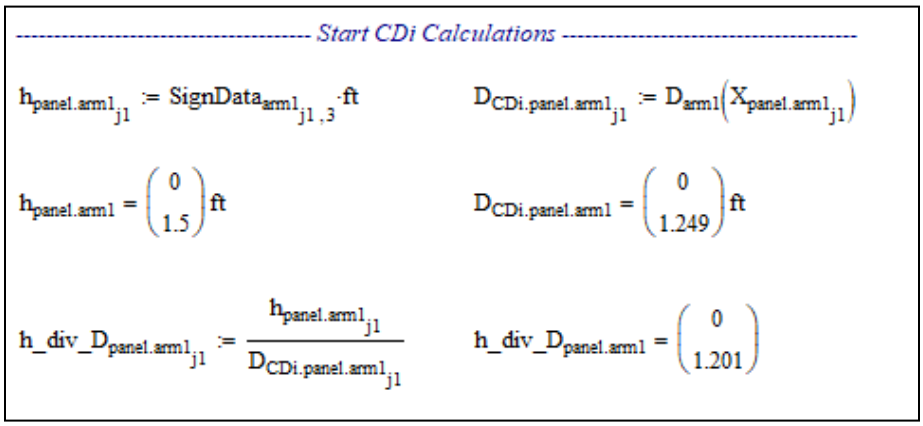

Figure 4-5. Individual geometric ratio (*h/D*) determination for signs

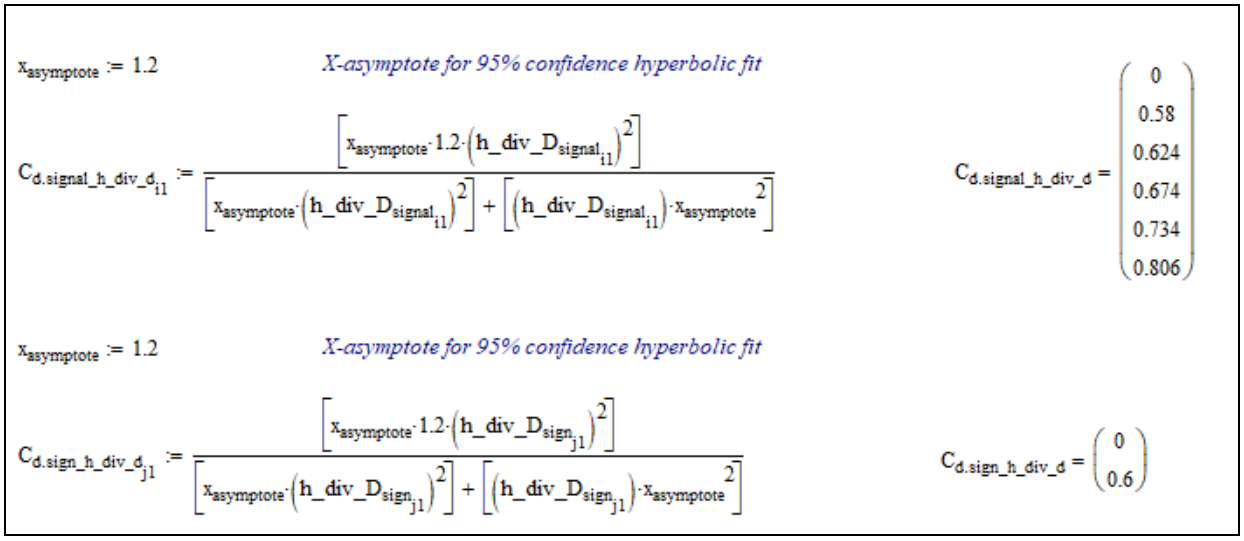

Figure 4-6. Individual C_{di} determination for signals (top) and signs (bottom)

4.3. Implementing Proposed Analytical Modifications: Definition of Three Studies

The proposed analytical modifications were implemented into the FDOT Mast Arm program to investigate their influence on base reactions (over-turning moment, torsion, and along-wind shear) for complete mast arm structures with signal systems. Base reactions resulting from the current method were compared to those resulting from the proposed method.

The first study investigated the ability of the incremental drag coefficient approach to distinguish between horizontal and vertical signal orientation. The reactions at the base were obtained using only the incremental drag coefficient (C_{di}) modification, rather than both C_{di} and the height and exposure factor (K_Z) modifications. The presence of back plates was assumed in both the unmodified and modified calculations. Modified calculations were conducted for both horizontal and vertical orientations. The modified reactions were normalized by those from the current method using horizontal orientation with back plates.

The second study investigated the influence of the proposed analytical modifications (C_{di} and Kz) individually and in combination. The orientation and configuration of the attachments were the same as in the unmodified (normalizer) and modified calculations: horizontal signals with back plates.

The third study included the effects of implementing the proposed analytical modifications when adding back plates to horizontal signals. Base reactions were determined from the current FDOT Mast Arm program for horizontal signals with back plates, and from the parameter-modified program for horizontal signals with back plates. These were then normalized by base reactions from the current method without back plates. This approach provides a ratio of loads on back plate systems using the parameter-modified program to the loads on otherwise identical but no-back plate systems using the current program. This comparison is most relevant to the use of the parameter-modified program to determine whether adding back plates to existing systems would result in capacity exceedance.

The comparative base reactions between the current and modified methods are presented in a normalized framework. Each reaction (over-turning moment, torsion, and along-wind shear) produced by the parameter-modified program was normalized by the corresponding base reaction from the current FDOT Mast Arm program. Next, the three normalized reactions were averaged together. For each mast arm the normalized reactions (moment, torsion, and shear) were found to be of similar magnitude, indicating that each average value was a reasonable metric for comparing the current and modified methods. A normalized value less than 1.0 indicates that the modification produced a reduction in the average of the base reactions, relative to current FDOT practice.

Mast arms chosen for investigation were Mast Arm 1 (Figure 2-1), Mast Arm 7 (Figure 2-7), and Mast Arm 9 (Figure 2-9). These mast arms were chosen based on their size, with Mast Arm 1 being the largest, Mast Arm 9 being the smallest, and Mast Arm 7 being an approximate median. Signs were present in the investigation in accordance with the mast arm drawings. To maintain consistency with current FDOT specifications, a 6-inch wide back plate was used in the following calculations.

4.4. Implementing Proposed Analytical Modifications: Results of Three Studies

Figure 4-7 through Figure 4-9 represent results from the three studies. As discussed above, the values on the plots represent averaged normalized reactions at the base of the structure. In Figure 4-7 and Figure 4-8 the modified base reactions are normalized by the base reactions determined using the current FDOT Mast Arm program for horizontal signals with back plates. In Figure 4-9 the reactions are normalized by reactions for horizontal signals with no back plate, determined using the current FDOT Mast Arm program. In all three figures, a value less than one indicates a reduction in the calculated base reactions relative to the current design approach.

Figure 4-7 presents the results of the incremental drag coefficient approach to distinguish between horizontal and vertical signal orientation (study one). Figure 4-7 illustrates that the use of C_{di} to account for signal orientation and the effects of partial shielding provides a reduction in base reactions over the current approach. For all three mast arms, vertical signal orientation resulted in higher reactions compared to horizontal signal orientation due to a higher h/D yielding a higher C_{di} value. This is consistent with the fact that less of the mast arm is shielded when the signal is in the vertical orientation. The reduction in loads for horizontal signal orientation was approximately 15-18%, while the vertical signal orientation resulted in load reductions of approximately 10-12%.

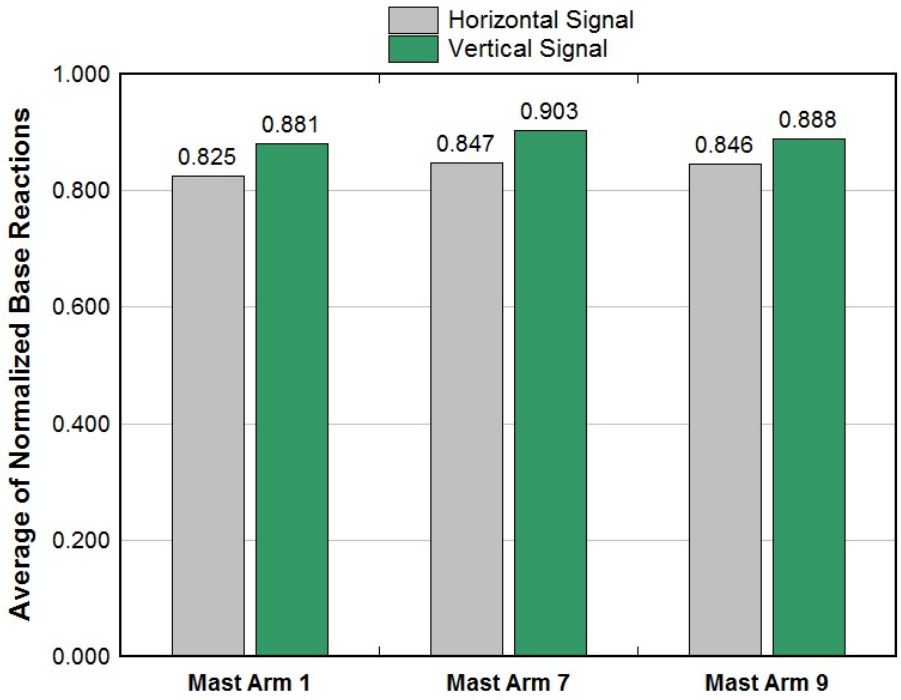

Figure 4-7. Study one: The influence of the incremental drag coefficient with respect to signal orientation (vertical or horizontal). Signals with back plates. K_Z modification not included. Normalized by current design loads with back plates

Figure 4-8 presents the resultant influence of the proposed analytical modifications individually and in combination (study two). The first (left) set of bars show the effect of implementing both proposed modifications (C_{di} and K_Z). The second and third sets of bars indicate the contribution to load reduction provided individually by C_{di} and K_Z, respectively. Adjusting K_Z alone yields a small load reduction (approximately 6-7%), while adjusting C_{di} alone yields more significant load reduction (approximately 15-18%). Adjusting both parameters yields combined load reductions of approximately 20-22%.

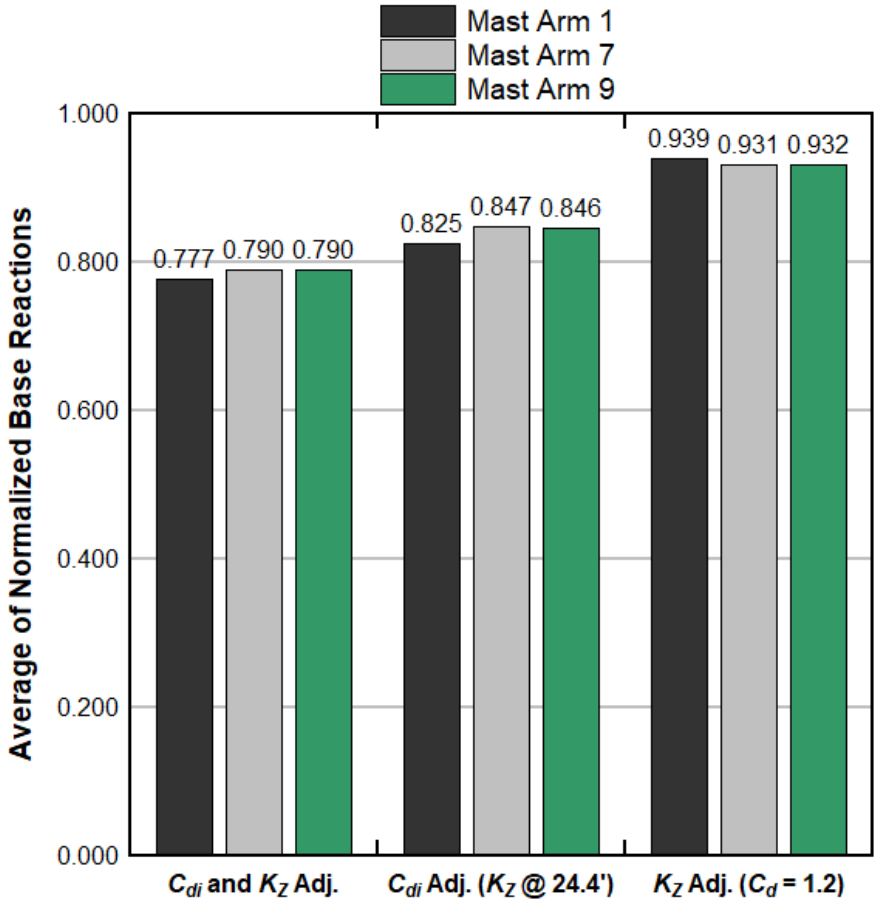

Figure 4-8. Study two: The influence of implementation of the proposed modifications individually and in combination. All reactions from horizontal signals with back plates. Normalized by current design loads with back plates

Figure 4-9 presents the resultant influence of implementing the proposed analytical modifications when adding back plates to horizontal signals (study three). The results show that the addition of back plates to signals using current design approach adds a significant amount of load to the structure (left solid bar in each pair). An increase of nearly 40% can be seen for Mast Arm 1, while Mast Arm 9 sees an increase of close to 50%. The right solid bar in each pair shows the resultant load ratio of a back plate system (modified-parameter program) to the no-back plate system (current FDOT program). The hatched regions quantify the influence of the individual modifications in producing the solid right bar. With the implementation of the proposed modifications to signals with back plates, loads are reduced by approximately 30% in each case (Mast Arm 1: 1.37 → 1.06, Mast Arm 7: 1.41 → 1.11, Mast Arm 9: 1.46 → 1.15).

Despite the significant load reductions offered by the two proposed parameter modifications, these results show that using the parameter-modified program to add back plates to systems currently at capacity (as defined by current FDOT program) still result in capacity exceedance. This outcome motivates the next phase of the investigation: Hardware Modifications.

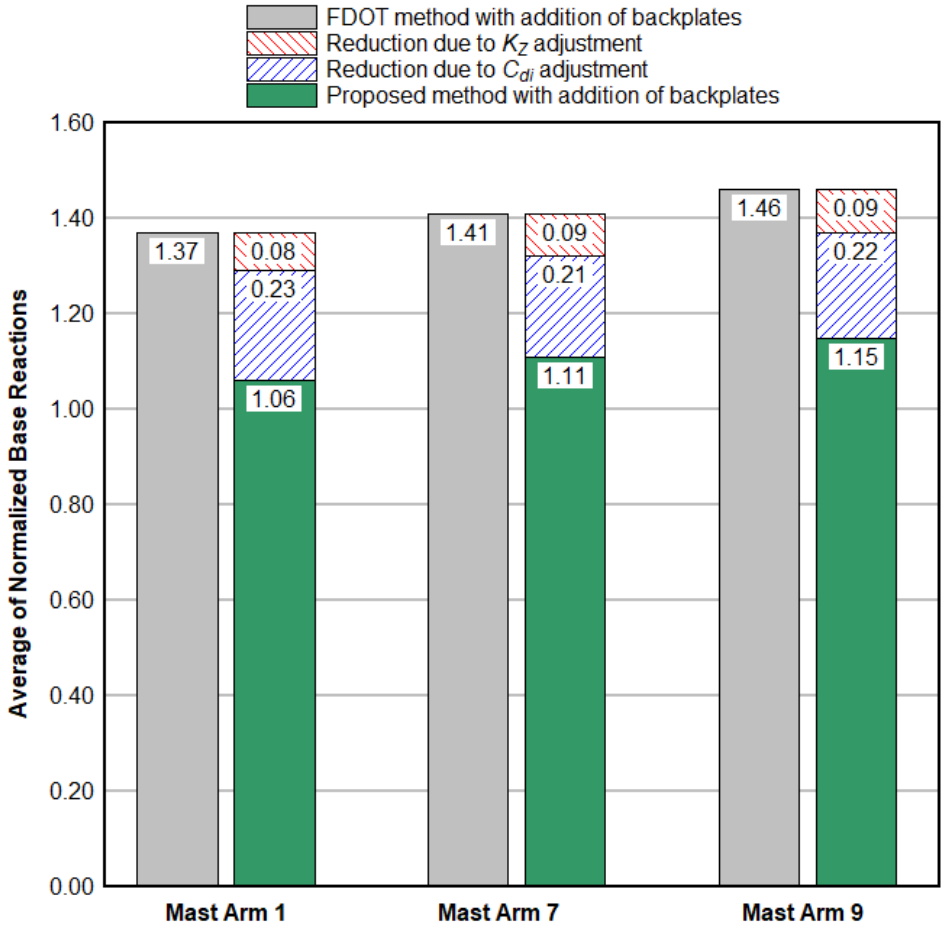

Figure 4-9. Study three: The effect of adding back plates to horizontal signals using the proposed modifications. Normalized by current design loads without back plates

5. Proposed Hardware Modifications

5.1. Overview

This section provides eight concepts for modifications to traffic-related hardware. The goal of the modifications is to provide a reduction in the wind loads acting on the mast arm structure. The proposed hardware modifications are presented in three separate groups: area reduction modifications, flow alteration modifications, and flexible/permeable/louver modifications.

5.2. Proposed Area Reduction Modifications

From the equation for wind-induced forces introduced in Section 1 ($F = P_Z \cdot A$), it can be seen that by reducing the projected area of the attachment, wind loads due to the given attachment decrease proportionally. Area reduction modification, however, would require manufacturing modifications to existing back plates and periodic maintenance to ensure proper operation.

5.2.1. Foldable Back Plates

Foldable Back Plate modifications would be created by adding hinges with rotational springs along horizontal edges of back plates at the location where they meet the signal (Figure 5-1). The hinged portion of the back plate would fold under design wind loads, backward or forward dependent on wind direction, and lock into position. This modification, however, would require personnel to manually unlock back plates back into upright position after a wind event.

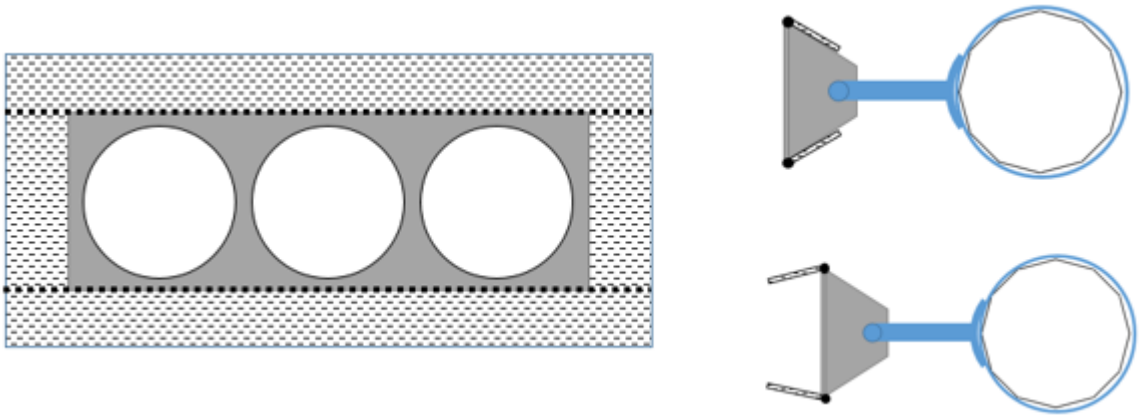

Figure 5-1. Front and side elevation view of signal with Foldable Back Plates modification

5.2.2. Magnetized Foldable Back Plates

Magnetized Foldable Back Plates would have modified back plates with hinged panels that would rotate under design wind loads to allow wind to pass through the back plate (Figure 5-2). A pair of magnets (one on the movable piece, and one on the back plate) would keep the hinged piece in its normal operating position during low wind speeds. A rotational spring would be incorporated to enable the rotating panels to return to the original vertical position automatically after the storm

event. This modification would not require personnel to manually return back plates to their normal operating position configuration. However, routine inspection and testing of the mechanism would be required to ensure proper operation during extreme wind events.

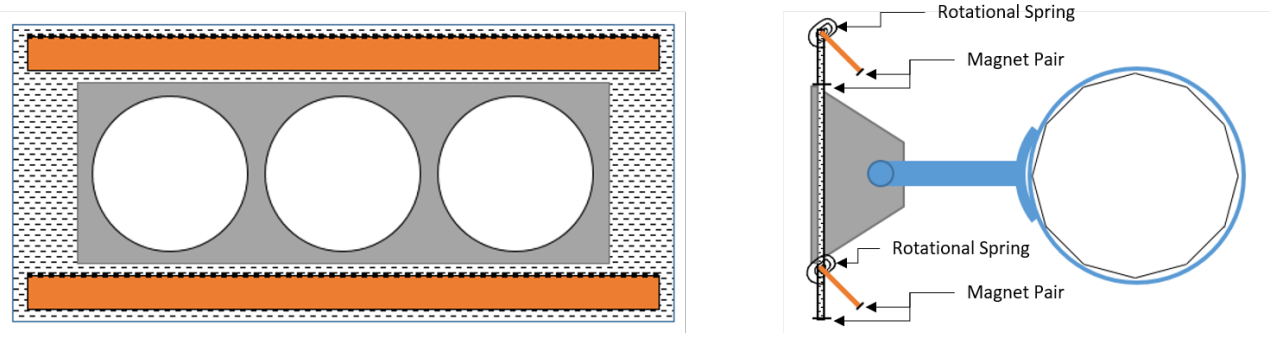

Figure 5-2. Front and side elevation view of signal with Magnetized Foldable Back Plates modification

5.2.3. Pinwheel

Pinwheel modifications would have modified back plates with panels that would rotate on a horizontal shaft under wind loads (Figure 5-3). The fins of the Pinwheel modification would be angled to visually mimic the appearance of louvers, and allow wind to pass through. The pinwheel modification has the benefit of providing a back plate with high conspicuity during wind events, and low maintenance. However, it may present possible acoustic considerations (such as whistling during wind events). Further, the motion of the pinwheel in windy but non-extreme wind events may distract the attention of motorists rather than serve its purpose of drawing attention to the signal. Finally, quantifying the reduction in wind loading would require full scale testing beyond the scope of this study.

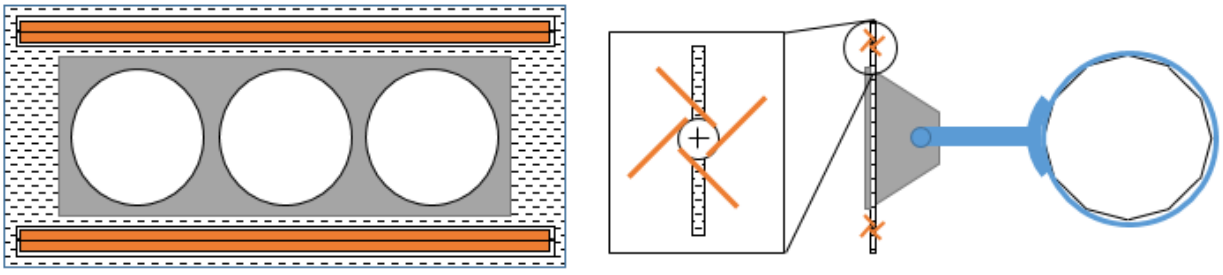

Figure 5-3. Front and side elevation view of signal with Pinwheel modification and blow-up of pinwheel modification

5.3. Proposed Flow Alteration Modifications

Flow Alteration modifications can be achieved by affixing offset covers between the attachment and the mast arm, thus allowing for smoother transition of flow between back plate and mast arm. This load reduction mechanism would be quantified by observing a decrease in the incremental drag coefficient (C_{di}). Flow alteration offers the benefit of not requiring any modification to existing back plates, and being easy to install. However, it has the potential to increase vertical forces, and provides a "shelf" for debris, water, and animals to accumulate if the ends are not closed.

5.3.1. Offset Cover

Offset Cover modification would have thin aluminum plates attached from horizontal edges of back plate to top and bottom edges of mast arm (Figure 5-4). The plates would be either clipped or bolted to the back plates. At the mast arm, the connection would be made using ring clamps that feed through slots in the plate to hold it in place. The lower plate would have perforations to enable drainage.

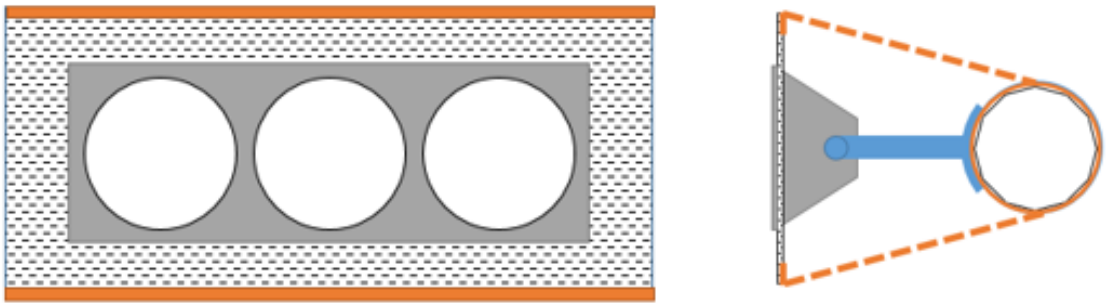

Figure 5-4. Front and side elevation view of signal with Offset Cover modification

5.3.2. Chamfer

The Chamfer modification would be created in similar fashion to the Offset Cover, bolting thin aluminum plates from horizontal edges of back plate that extend back towards the arm (Figure 5-5). The plates, however, would be slightly curved allowing wind to flow over and around the signal.

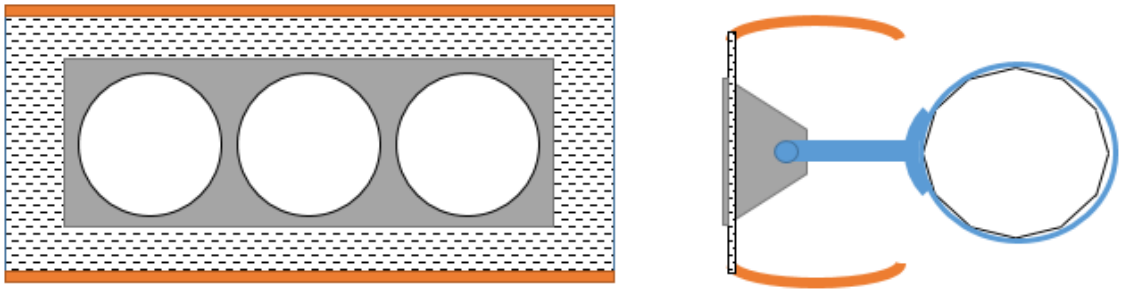

Figure 5-5. Front and side elevation view of signal with Chamfer modification

5.4. Proposed Flexible/Permeable/Louver Modifications

Flexible/Permeable/Louver back plate modifications would allow for wind to flow through portions of the back plate with limited resistance. The Permeable modifications differ from area reduction modifications by the amount of area reduction. Permeable modification may be achieved, for example, by creating a wireframe back plate, whereas area reduction modifications are achieved by removing large blocks of area. Wind load reduction in the Permeable modification would not be directly proportional to the modified area. All three modifications under this section would require low maintenance, however manufacturing modifications to existing back plates would be required. Additionally, Louver modification has the potential to generate either uplift or downdraft forces (depending on flow direction) as wind flows through the angled louvers.

5.4.1. Flexible Modifications

The Flexible modification would incorporate fibers on the long sides of the back plate that would bend and sway in the wind while still providing conspicuity (Figure 5-6).

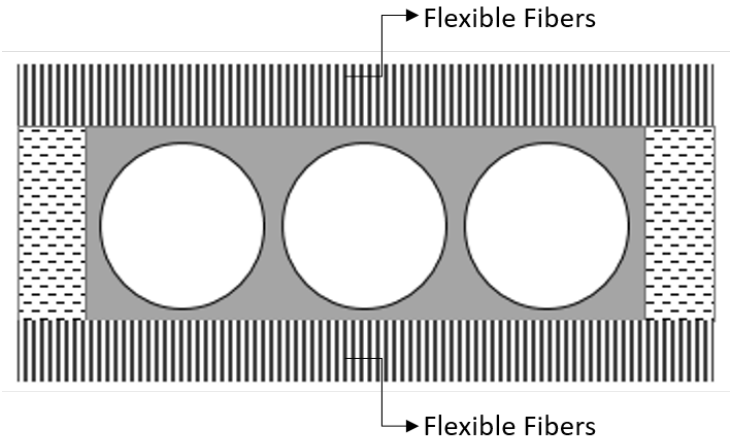

Figure 5-6. Front elevation view of Flexible modification

5.4.2. Permeable Modifications

Permeable modification would use a wireframe back plate which, similar to the Flexible modification, would allow for wind to flow through while providing adequate conspicuity (Figure 5-7).

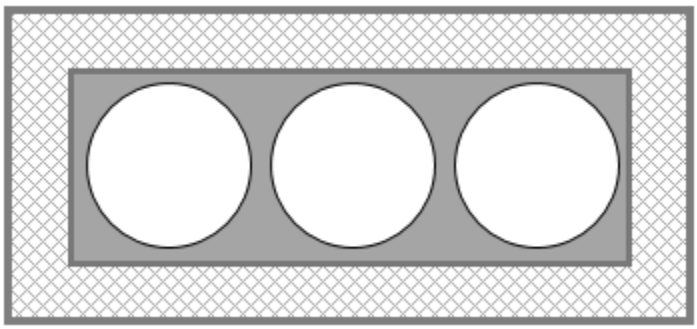

Figure 5-7. Front elevation view of Permeable modification

5.4.3. Louver Modifications

Louver modification would be created by incorporating large louvers that extend the entire length of the back plate (Figure 5-8). Louvers would be positioned in such way that they would appear opaque when viewed from street level while allowing some airflow to pass through.

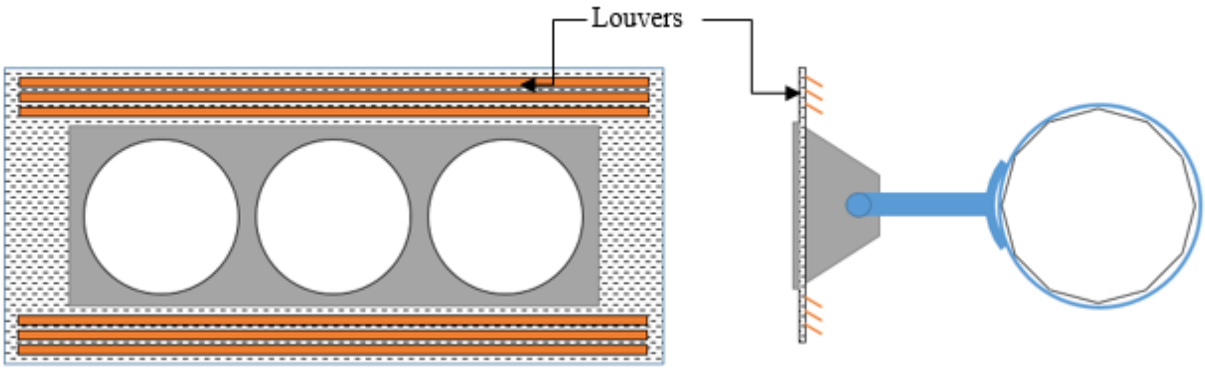

Figure 5-8. Front and side elevation view of signal with Extended Louver modification

6. Performance Evaluation of Proposed Hardware Modifications

To study the potential benefits of proposed hardware modifications, a third phase of wind tunnel testing was conducted. Not all of the proposed signal hardware modifications presented in Section 5 are suitable for testing in a reduced-scale testing environment. This section focuses on the testing and evaluation of proposed hardware modifications that are suitable for reduced-scale model testing. This section also provides a discussion of the results from wind tunnel testing, as well as results from implementing tested hardware modifications into the FDOT Mast Arm program.

6.1. Overview

The influence of proposed hardware modifications based on very small back plate openings, or that employ flexible or permeable materials, are not expected to be accurately quantified at the scale of the tests performed in the wind tunnel (1:20–1:8 scales). Modifications that are the result of large back plate area removal, or alterations to the wind flow path, are more likely to yield meaningful results in reduced-scale testing. As a result, signals with a slotted back plate (back plate with a gap) were tested as a simplified representation of the Pinwheel and foldable back plate modifications. Signals with offset cover were also tested. Analysis of the results demonstrate that load reduction measured at model scale could be reasonably scaled up to a full scale attachment. The Large Louver, Flexible, and Permeable modifications were not tested due to scaling issues.

6.2. Hardware Modification Testing

This section discusses the testing methodology and procedures used to analyze test data. Results are discussed along with the potential benefits of each proposed hardware modification.

6.2.1. Wind Tunnel Testing Method

The testing methodology for the hardware modifications was similar to that of the Supplementary Testing. Tests were conducted on a single traffic signal or modified traffic signal on a single vertical pole at a geometric scale of 1:8. As in earlier phases of testing, two different dodecagon cylinder pole diameters were considered—one representing the largest pole diameter from the representative mast arms, and the other representing the smallest pole diameter. Attachments were tested in both horizontal (parallel to pole) and vertical (perpendicular to pole) configurations. The test matrix for the modified attachments is shown in Table 6-1.

The Slotted modification is a simplified representation of the three area reduction modifications (Pinwheel, Magnetized Foldable back plates, and Foldable back plates). The Slotted modification was modeled by creating an aluminum back plate with cutout slots (Figure 6-1a). The slotted back plate was then fitted behind a 3D printed signal. Dimensions of the slot were chosen in such a way as to yield maximum area reduction while allowing for proper manufacturing of the back plate. Dimensions of the slot were, at reduced-geometric scale, 5.85”x0.4375” (LxW), yielding an area reduction of 28% relative to a solid back plate system. There was some initial concern that the presence of the thin strips of back plate at the top and bottom of the modified attachment would result in flow conditions at the model scale that may not represent flow conditions at full scale. To address this potential issue, a second back plate modification model was created with the purpose of checking that the area reduction of the tested Slotted modification was being accurately captured at model scale. This second modification (henceforth referred to as

Dogbone) was similarly created out of aluminum plates with dimensions chosen to produce the same area reduction as that of the Slotted modification. However, the thin perimeter material running along the length of the slots was removed in order to mitigate potential Reynolds number sensitivity that the scaled slots may introduce (Figure 6-1b).

Table 6-1. Test matrix for Hardware Modification phase of wind tunnel testing

Test ID	Model Description	Attached Signal
CYL1_A	2.125” Dodecagon Cylinder	None
CYL2_A	0.325” Dodecagon Cylinder	None
CYL1_B	2.125” Dodecagon Cylinder	Parallel w/ Slotted Modification
CYL2_B	0.325” Dodecagon Cylinder	Parallel w/ Slotted Modification
CYL1_C	2.125” Dodecagon Cylinder	Perpendicular w/ Dogbone Modification
CYL2_C	0.325” Dodecagon Cylinder	Perpendicular w/ Dogbone Modification
CYL1_D	2.125” Dodecagon Cylinder	Perpendicular w/ Slotted Modification
CYL2_D	0.325” Dodecagon Cylinder	Perpendicular w/ Slotted Modification
CYL1_E	2.125” Dodecagon Cylinder	Parallel w/ Dogbone Modification
CYL2_E	0.325” Dodecagon Cylinder	Parallel w/ Dogbone Modification
CYL1_F	2.125” Dodecagon Cylinder	Parallel w/ closed Enclosed Modification
CYL2_F	0.325” Dodecagon Cylinder	Parallel w/ closed Enclosed Modification
CYL1_G	2.125” Dodecagon Cylinder	Parallel w/ open Enclosed Modification
CYL2_G	0.325” Dodecagon Cylinder	Parallel w/ open Enclosed Modification
CYL1_H	2.125” Dodecagon Cylinder	Unmodified Parallel
CYL2_H	0.325” Dodecagon Cylinder	Unmodified Parallel
CYL1_I	2.125” Dodecagon Cylinder	Perpendicular w/ closed Enclosed Modification
CYL2_I	0.325” Dodecagon Cylinder	Perpendicular w/ closed Enclosed Modification
CYL1_J	2.125” Dodecagon Cylinder	Perpendicular w/ open Enclosed Modification
CYL2_J	0.325” Dodecagon Cylinder	Perpendicular w/ open Enclosed Modification
CYL1_K	2.125” Dodecagon Cylinder	Unmodified Perpendicular
CYL2_K	0.325” Dodecagon Cylinder	Unmodified Perpendicular

Test ID Key		
Support_Attachment	Support	
	CYL1	Larger Dodecagon Cylinder
	CYL2	Smaller Dodecagon Cylinder
	Attachment	
	A to K	Various signals as described in column 3 above

Each configuration in the test matrix was tested with a 1.25 inch offset between the attachment and the pole since it was shown during Supplementary Testing that the results were not affected by differences in signal offsets. The tests were conducted at a wind speed of 15 m/s. Each configuration was tested at 0° orientation (signal facing approaching flow), and 180° orientation (signal facing opposite of approaching flow) with two trials per direction at two minutes of testing per trial.

(a) (b)

Figure 6-1. Area reduction hardware modifications on small cylinder: (a) Slotted modification; (b) the Dogbone modification that acts as check to Slotted modification

Flow alteration modifications (fully enclosed and partially enclosed) were modeled using cardboard to shield the gap between the attachment and the pole. In the fully enclosed modification, duct tape was used to stiffen and hold the cardboard in place, as well as completely seal the region around the pole (Figure 6-2a). Also tested was a Partially Enclosed modification in which both ends were left open. The openings were always on the sides perpendicular to the pole (Figure 6-2b). An unmodified signal attachment with back plate was tested to act as check that this phase of testing matched previously conducted experimental testing, and to serve as a baseline for comparison between the modified and unmodified signal attachments.

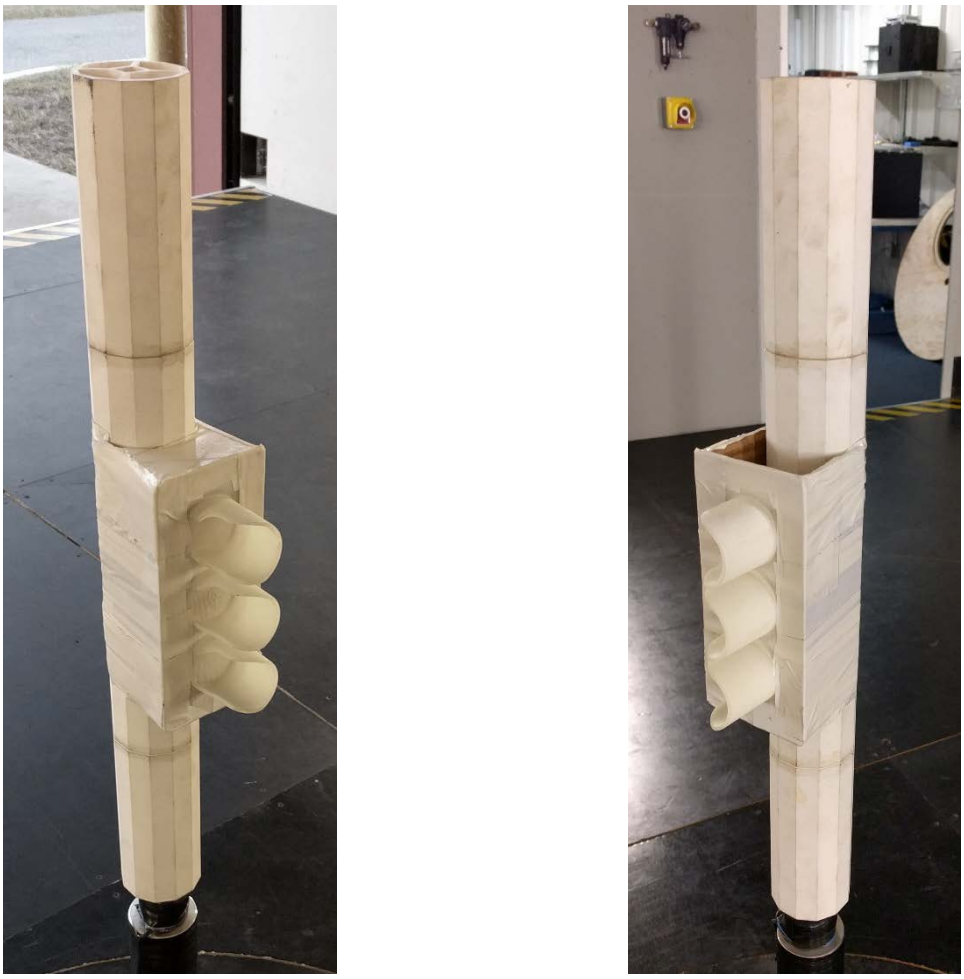

(a) (b)

Figure 6-2. Flow-alteration hardware modifications: (a) Fully Enclosed Modification on large cylinder; (b) Partially Enclosed Modification on large cylinder

6.2.2. Analysis Approach

Slotted Modifications

For the area reduction modifications (Slotted and Dogbone), the approach taken was to quantify the proportionality of load reduction to area reduction. At full scale for bluff bodies this proportionality should be a 1-to-1 ratio. To quantify the experimentally determined proportionality, the ratio of percent load difference from unmodified to modified and the percent area difference from unmodified to modified were calculated, denoted as area reduction factor α:

$$\alpha = \frac{\frac{R_U - R_M}{R_U}}{\frac{A_U - A_M}{A_U}} \tag{6}$$

where R_U is the reaction from the unmodified signal attachment, R_M is the reaction from modified signal attachment, A_U is the projected area of the unmodified signal, and A_M is the projected area of the modified signal. A value of $\alpha = 1$ indicates a 1:1 proportional reduction in load with reduction in area, whereas $\alpha < 1$ indicates that the load was reduced by an amount less than a 1:1 proportion would indicate. To isolate the reactions due to the signal attachment alone, the unshielded portions of the pole were deducted from the composite values (i.e., pole plus signal). Figure 6-3 illustrates this calculation procedure. The following steps outline the procedure that was used to isolate reactions attributable to the signal attachment:

1. Base reaction values (along-wind shear, and over-turning moment) for bare pole are experimentally determined (R_{BP})
2. Base reaction values for pole with attachment (composite) are experimentally determined (R_C)
3. Projected area of the bare pole (A_{BP}) is calculated using $A_{BP} = D_{pole}*H_{pole}$, where D_{pole} is pole diameter and H_{pole} is pole height
4. Projected area of the unshielded (exposed) portion of pole is calculated using dimensions of attachment, and bare pole (A_{pole_exp})
5. Base reaction for bare pole (R_{BP}) is multiplied by the ratio of exposed (i.e., unshielded) pole area (A_{pole_exp}) to bare pole area (A_{BP}) yielding reaction values from unshielded portion of pole (R_{BP_exp})

$$R_{BP\_exp} = R_{BP} \times \frac{A_{pole\_exp}}{A_{BP}} \quad (7)$$

6. Reaction values for the signal alone are then determined, separately for shear and moment, by: $R = R_C - R_{BP\_exp}$. For the unmodified case $R = R_U$, and for the modified case $R = R_M$

Once shear and moment reactions for signals were isolated, α values corresponding to these reactions were calculated, then averaged together in order to obtain a final α value for each of the Slotted and Dogbone modifications. To calculate attachment loads, unmodified projected areas were replaced by αA_M to yield: $F_M = \alpha A_M * P_Z$, where F_M is the load due to modified attachment, α is load-to-area proportionality factor, A_M is the projected area of the modified signal, and P_Z is design wind pressure.

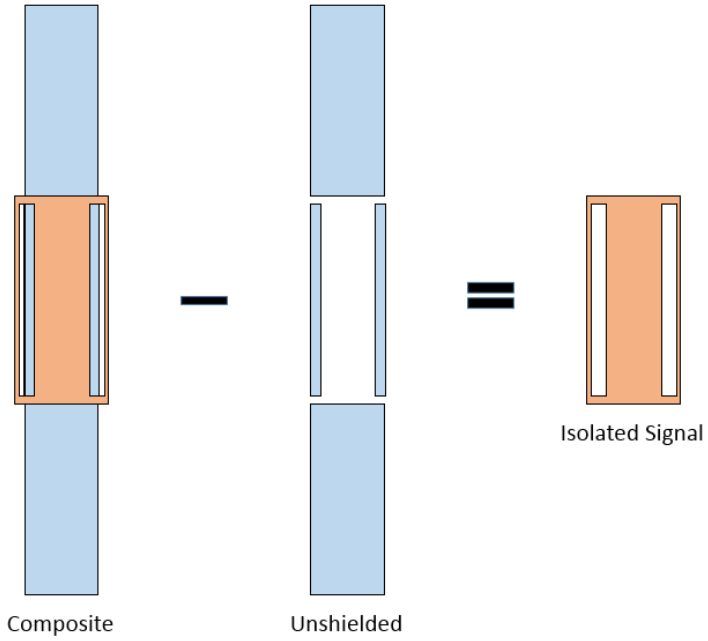

Figure 6-3. Representative illustration of calculation procedure to isolate reactions due to signal alone

Enclosed Modification

The analysis approach that was applied to the Enclosed modification involved calculating C_{di} values from wind tunnel testing and then comparing them to the C_{di} results reported in Section 3.3.2 for unmodified signals. Since the loading mechanism in the Enclosed modification was flow alteration, a further decrease in C_{di} would be indicative of additional load reduction (shielding) from the modification.

6.2.3. Results of Hardware Modification Testing

Results presented in this section are for 0° direction tests. During data analysis, it was observed that measured reactions for tests conducted at 180° were consistently smaller than those measured for tests at 0°. Thus, the 0° results constitute the more conservative case. Furthermore, there were concerns that at 180°, measured forces could be Reynolds number sensitive due to the wind coming into contact first with the pole—a streamlined body at a reduced-geometric scale of 1:8. Results for tests conducted at 180° were therefore omitted.

Slotted Modification

Alpha value for each tested configuration (e.g., perpendicular Slotted on small cylinder) was calculated, then grouped by hardware modification (Slotted or Dogbone) and averaged together to obtain an average alpha (α_{avg}) value for each modification. Figure 6-4 shows the average alpha values for the Slotted and Dogbone modifications, with unmodified signals shown for comparison.

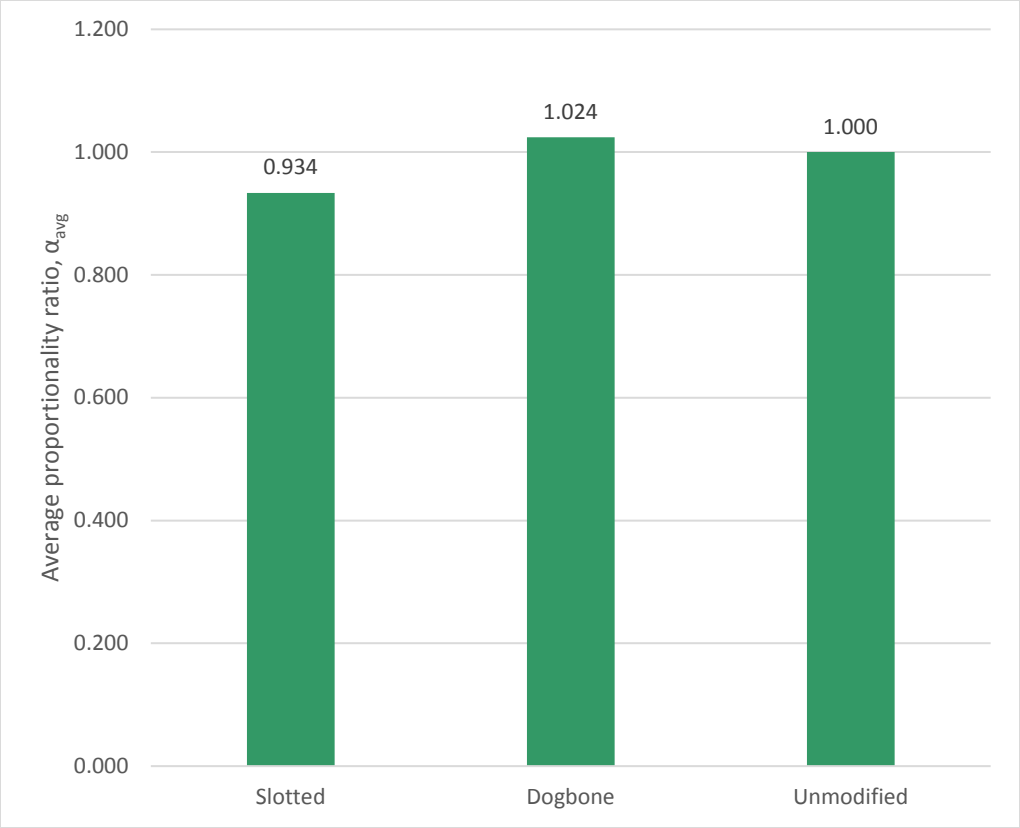

Figure 6-4. Average of proportionality ratio (α_{avg}) for modified and unmodified signal attachment

A value of α equal to 1.0 indicates 1-to-1 proportionality between load reduction and area reduction. From Figure 6-4, it can be seen that the average α values for the Slotted modification (0.934) and Dogbone modification (1.024) were 6.6% smaller and 2.4% larger, respectively, than the reference. The slightly larger percent difference between Slotted and unmodified (vs. percent difference between Dogbone and unmodified) may be attributed to Reynolds number effect of air flowing through the slots at a geometric scale of 1:8. The Dogbone average α being slightly greater than 1.0 is likely due to uncertainties in the precision of experimental testing. In general, Figure 6-4 indicates that incorporating modified back plates, which alter (reduce) the projected area, may yield load reduction that is approximately proportional to the area reduction (i.e., $\alpha = 1$).

It is worth repeating that the experimentally tested Slotted modification is a *simplified* representation of the Pinwheel and Magnetized Slot modifications. It is expected that α would be less than 1.0 for such modifications due to drag on the pinwheel or flaps—influences not captured during testing. To capture the appropriate α values for these modifications, full scale testing, with inclusion of pinwheel and flap mechanisms, would be required.

Enclosed Modification

Figure 6-5 presents incremental drag coefficient (C_{di}) values obtained from wind tunnel testing of unmodified attachments (recall Figure 3-19), along with C_{di} values obtained from wind tunnel testing of the Enclosed modifications.

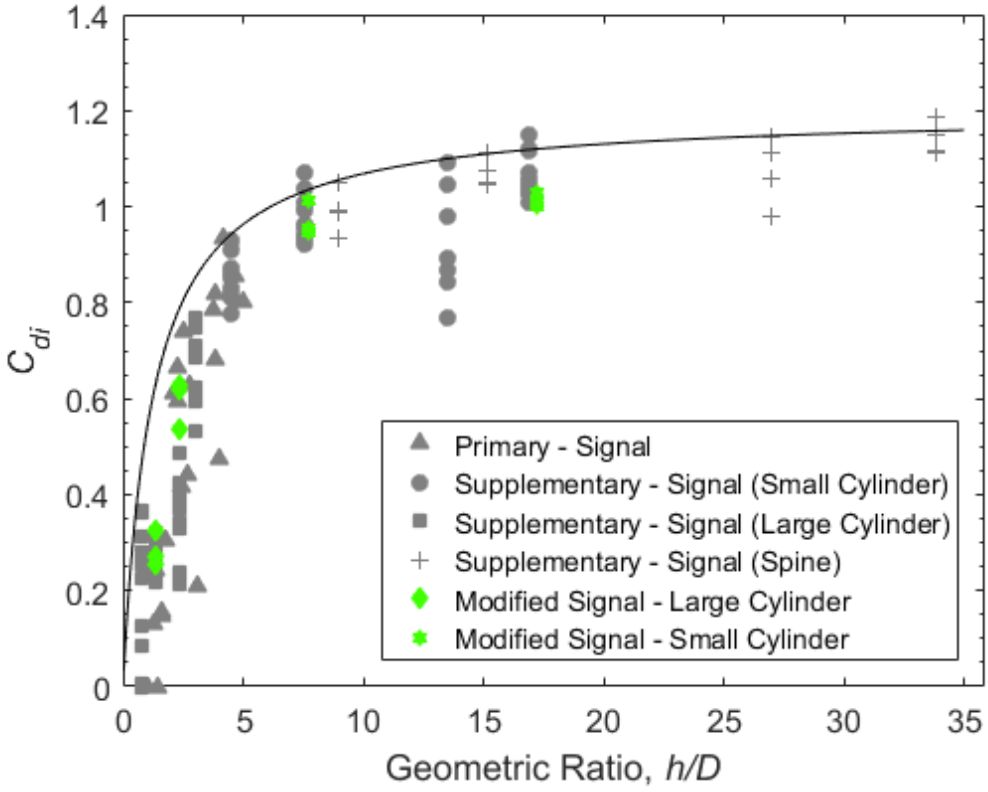

Figure 6-5. Signal incremental drag coefficient (C_{di}) versus geometric ratio (h/D)—Primary, Supplementary, and Hardware Modification Testing

From Figure 6-5 it can be observed that the C_{di} values for the Enclosed modifications fall within the spread of data from previous phases of testing, indicating no measurable load reduction from adding offset covers to currently employed signals with back plates.

6.3. Implementation of Results of Hardware Modification Testing

Results obtained from analysis of the wind tunnel test data were implemented into the FDOT Mast Arm program to investigate the influence of the proposed Slotted modification on base reactions (over-turning moment, torsion, and along-wind shear) for complete mast arm structures with signal systems.

6.3.1. Analysis Approach

First investigated was the effect of implementing the proposed Slotted modification (considering area reduction but ignoring K_Z and C_{di} reductions) to mast arms containing signals

with back plates. The base reactions calculated were compared to base reactions resulting from the parameter-modified FDOT Mast Arm program and those resulting from area-modified FDOT Mast Arm program.

The investigation was then expanded to analyze the effects of superimposing the proposed modifications (K_Z, C_{di}, and α) when adding back plates to horizontal signals. The effects of adding back plates using the current FDOT Mast Arm program were compared to the effects resulting from the parameter-modified plus area-modified FDOT Mast Arm program.

Similar to Section 4.3, to quantify changes between methods (i.e., current approach, parameter-modified, area-modified, and parameter-modified plus area-modified), the comparative base reactions between the methods are presented in a normalized framework. Each reaction produced by one of the modified methods was normalized by the corresponding base reaction from the current FDOT method. Next, the three normalized reactions (moment, torsion, and shear) were averaged together. For each mast arm, these normalized reactions were found to be of similar magnitude, indicating that each average value was a reasonable metric for comparing the current and modified methods.

Mast arms chosen for investigation were the same as those used in Section 4.3: Mast Arm 1 (Figure 2-1), Mast Arm 7 (Figure 2-7), and Mast Arm 9 (Figure 2-9). These mast arms were chosen for the same reasons laid out in Section 4.3. Signs were present in the investigation in accordance with the mast arm drawings. To maintain consistency with current FDOT specifications, a 6-inch wide back plate was used in the following calculations.

6.3.2. Findings from Implementation of Results

Figure 6-6 and Figure 6-7 present results of the two investigations. The values in the plots represent averaged normalized reactions at the base of the structure. For each bar plot, a value less than 1.0 indicates a reduction in the calculated base reactions relative to the current FDOT design approach.

Figure 6-6 presents the results of implementing the proposed Slotted modification. The first (left) set of bars shows the effect of implementing only the proposed parameter modifications from Section 4, namely C_{di} and K_Z. The second (middle) set of bars shows the effect of implementing only area reduction (with α = 1.0) associated with signal modifications. The last (right) set of bars shows the effect of implementing all three modifications together. It can be observed that incorporation of the Slotted modification alone yielded a load reduction of approximately 13-14%. The combination of C_{di}, K_Z, and area reduction yielded a load reduction of approximately 31-34%.

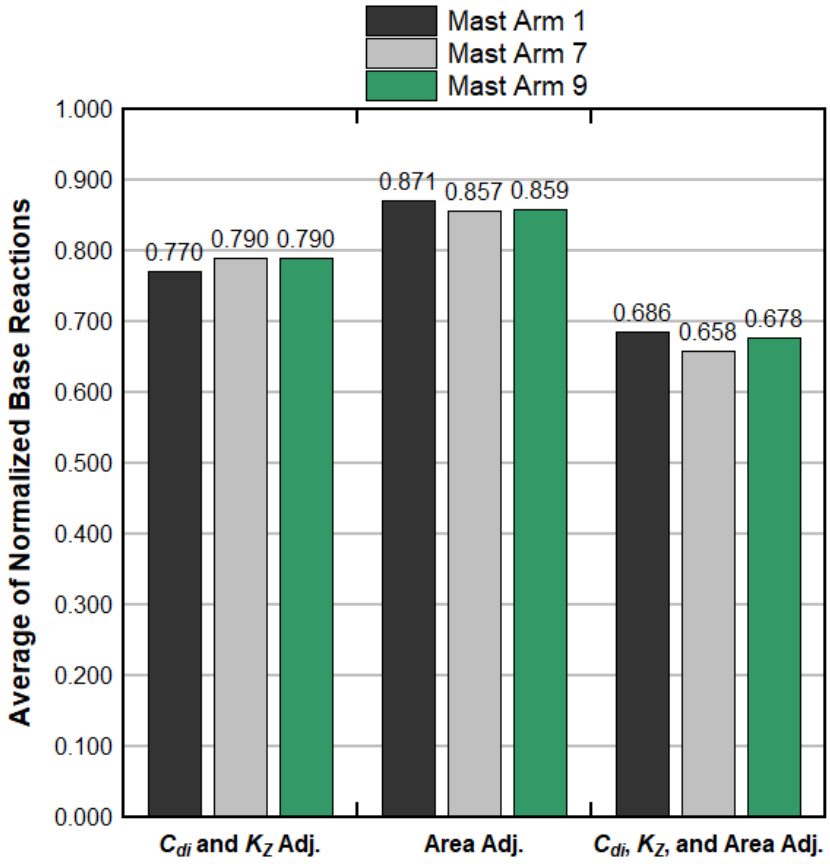

Figure 6-6. Influence of direct implementation of proposed hardware and parameter modifications. Normalized by current design loads with back plates

The description of Figure 6-6 follows the description of Figure 4-8, now with the additional area reduction modification. The results presented in Figure 6-7 show that, using the current FDOT design approach, the addition of back plates to signals increases base reactions experienced by the mast arm structure by 37% for Mast Arm 1, 41% for Mast Arm 7, and 46% for Mast Arm 9. Recall that in Section 4.4 it was reported that increases in base reactions associated with adding back plates could be mitigated by approximately 30% through adjustments to C_{di} and K_Z (Figure 4-9). The results in Figure 6-7 show that an area reduction (with $\alpha = 1.0$), due to the signal back plate modification, resulted in an additional 12% reduction on base reactions for Mast Arm 1, and 19% for Mast Arms 7 and 9. With the implementation of the proposed three modifications to signals with back plates (back plate area modification, C_{di} and K_Z), loads are reduced by 43% - 50%.

These results show that using the parameter-modified program to add area modified back plates to systems currently at capacity (as defined by current FDOT program) results in loads that are below capacity. However, the results in Figure 6-6 are based on the assumption that the area load reduction factor $\alpha = 1$, which corresponds to a true transparent gap (a slot) in the back plate. The actual physical modifications represented by the slotted modification, all described in Section 5.2, will have modification factors $\alpha < 1$. This will result in load reductions less significant than

shown in Figure 6-6. Full-scale testing of each of the Section 5.2 area modifications are required to quantify the α specific for each one.

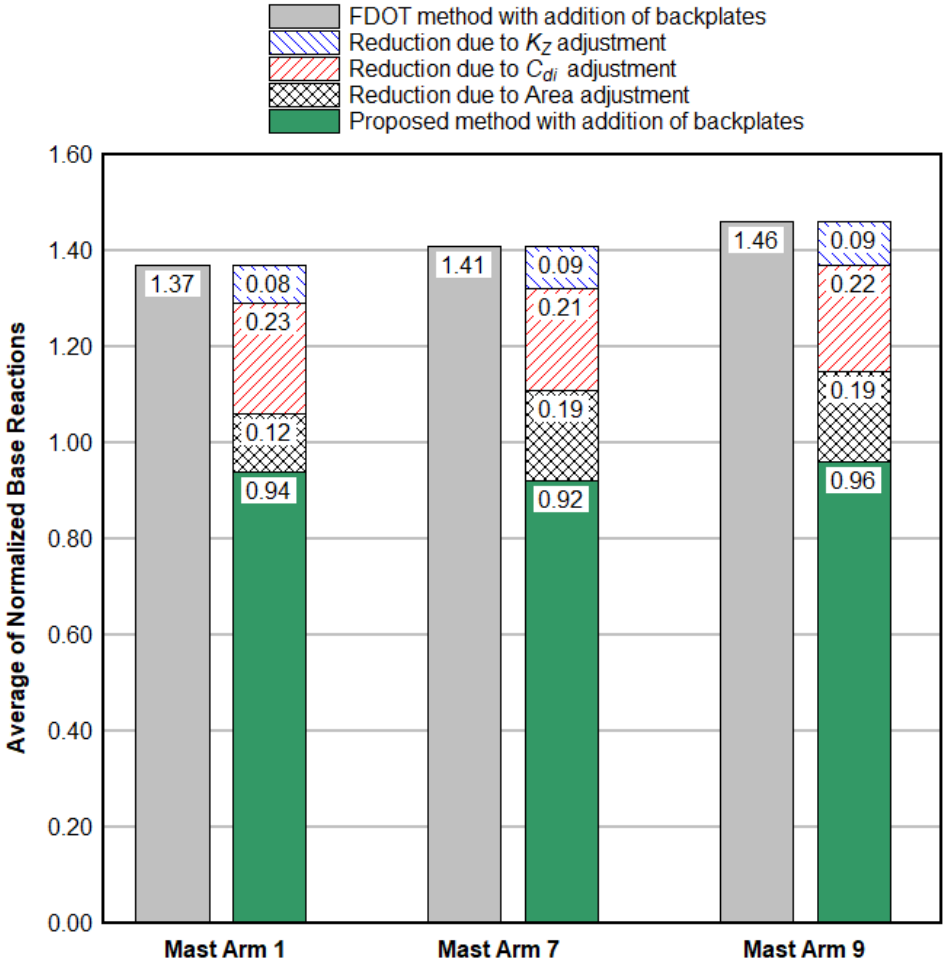

Figure 6-7. The effect of adding back plates to horizontal signals using the proposed modifications. Normalized by current design loads without back plates

6.4. Detailed Modification Drawing

Following data analysis of experimental testing results, the Slotted modification showed the most promise in decreasing global wind load reactions experienced by the mast arm. To illustrate an example of a Slotted modification, detailed drawings were generated for the Magnetized Slot modification. These detailed drawings may be found in Appendix B of this report.

7. Summary and Conclusions

In this study current procedures employed by the FDOT for analysis and design of mast arm structures were reviewed and experiments were conducted to identify residual mast arm system capacity. A collection of nine mast arm configurations was selected to represent mast arm designs commonly used in Florida, as well as those most often identified as being 'at capacity' based on the current design and analysis procedures. Findings from review and experimental testing indicate that selected parameters—Height and Exposure Factor, K_Z, and Drag Coefficient, C_d (specifically those applied to segments of the mast arm shielded by signals or signs)—used for wind-load calculations may be overly conservative. It was concluded that height-dependent calculations of K_Z, as opposed to the current calculation using a fixed height of 24.4 feet, could yield lower K_Z values, and therefore lower the design wind loads on the mast arm.

The Current FDOT design procedure calculates wind load on the entire mast arm using a drag coefficient appropriate for a mast arm directly exposed to approaching wind. Additional wind loads from attachments are calculated using an appropriate drag coefficient for attachments directly exposed to approaching wind. Global wind loads are determined by simple superposition, thus any reduced loading on the segments of the mast arm shielded by attachments is not accounted for. Experimental wind tunnel tests conducted in this study identified that load-reducing shielding of the mast arm does occur, and that the magnitude of the load reduction is related to the ratio of the attachment height to the mast arm diameter. It is proposed that the reduced wind load on the mast arm segments shielded by an attachment be implemented in design load calculations by reducing the drag coefficient on the attachment while continuing to fully load the mast arm as if unshielded. This reduced attachment drag coefficient is referred to as an incremental drag coefficient (C_{di}), as it represents the incremental difference in loading between a shielded and unshielded mast arm segment.

Implementation of proposed parameter modifications (K_Z and C_{di}) demonstrated that important structural demands (e.g., global wind load reactions) may be significantly reduced. Use of an incremental drag coefficient, C_{di}, determined for each individual attachment using the geometric ratio h/D, and a hyperbolic model of experimental data with a 95% envelope can reduce global wind load reactions by approximately 15-18%. Implementation of C_{di} also permits the orientation of signs and signals to be taken into account, resulting in lower loads (more shielding) for horizontally oriented attachments. Additionally, a K_Z value that is mast arm dependent (determined using the arm-to-pole connection height for given mast arm) can further reduce global wind load reactions. Load reductions resulting from use of the proposed parameter modifications (C_{di} and K_Z) were investigated for cases in which back plates were added to signals. The modified approach with signal back plates yielded base reactions that were 30% lower than reactions determined using the unmodified (current FDOT) approach with signal back plates.

In addition to design load parameter modifications, hardware modifications (Enclosed and Slotted) were developed and experimentally tested. Results from experimental testing of the Enclosed modification demonstrate that the addition of covers provide no load reduction compared to unmodified attachments. Results for the Slotted modification, however, showed that a reduction in the projected area of the back plate from folding or rotating panels yields an approximately proportional reduction in loads on the attachment. Results from the implementation of Slotted modifications into calculations of design load showed that by reducing the projected area of the attachment by approximately 30%, the global wind load reactions for the investigated mast arm structures decreased by approximately 13% for each of three different representative mast arm

configurations. Furthermore, the effects of implementing the proposed Slotted modification in conjunction with proposed parameter modifications (C_{di} and K_Z) was investigated. The results from the implementation of area reduction hardware modifications and parameter modifications demonstrated that important structural demands (e.g., global wind load reactions) may be reduced further compared to results from parameter modifications alone. Incorporating both the Slotted modification and parameter (C_{di} and K_Z) modification for signals with back plates yielded base reactions that were 43-50% lower than base reactions determined using current FDOT Mast Arm design for signals with back plates. However, this total load reduction is slightly larger than what should be expected in actual implementation, as it results from simplified area reduction experiments that used a true void (gap, slot). The actual physical modifications will not be a true void, and will therefore produce wind loads slightly higher than those measured in the simplified area reduction experiments. Full-scale testing of each of the area modifications are required to quantify the load reduction specific to each concept.

It is recommended that the proposed wind load calculation parameter modifications be applied to the analysis of existing mast arm structures to identify residual capacity and determine whether additional hardware can be added. The proposed modifications are not recommended for the design of new mast arm structures. The proposed modifications remove three conservative loading assumptions currently employed. Thus, designing new mast arm structures utilizing the proposed parameter modifications may result in mast arm structures that do not possess residual capacity for possible future hardware additions.

References

AASHTO. (2013). *Standard Specifications for Structural Supports for Highway Signs, Luminaires and Traffic Signals*, 6th Edition (LTS-6). American Association of State Highway and Transportation Officials. Washington, D.C.

AASHTO. (2015). *LRFD Specifications for Structural Supports for Highway Signs, Luminaires and Traffic Signals,* 1st Edition (LRFD-LTS-1). American Association of State Highway and Transportation Officials. Washington, D.C.

ADINA. (2016). *Theory and Modeling Guide, Volume 1: ADINA Solids & Structures*. ADINA R&D, Inc. Watertown, MA.

ASCE/SEI 7-10 Codes and Standards Committee. (2010). *Minimum Design Loads for Buildings and Other Structures*. American Society of Civil Engineers. Reston, Virginia.

ASCE Task Committee on Wind Forces. (1961). "Wind Forces On Structures". *Transactions of the American Society of Civil Engineers*. 126(2). 1124-1198.

Chen, G., Wu, J., Yu, J., Dharani, L.R., Barker, M. (2001). "Fatigue Assessment of Traffic Signal Mast Arms Based on Field Test Data Under Natural Wind Gusts", *Journal of the Transportation Research Board*. https://doi.org/10.3141/1770-24.

Consolazio, G.R., Edwards, S.T. (2014). *Determination of Brace Forces Caused by Construction Loads and Wind Loads During Bridge Construction*. Structures Research Report 2014/101350- 102056. Department of Civil and Coastal Engineering, University of Florida. April 2014. 115 pp.

Consolazio, G.R., Gurley, K.R., Harper, Z.S. (2013). *Bridge Girder Drag Coefficients and Wind-Related Bracing Recommendations*. Structures Research Report 2013/87322. Department of Civil and Coastal Engineering, University of Florida, June 2013. 230 pp.

Cook, R.A., Johnson, E.V., Ansley, M.H. (2007). *Development of Hurricane Resistant Cable Supported Traffic Signals*. Report No. BD545 RPWO #57. Department of Civil and Coastal Engineering, University of Florida. July 2017.

ESDU. (1986). *ESDU 80025: Mean Forces, Pressures and Flow Field Velocities for Circular Cylindrical Structures: Single Cylinder with Two-Dimensional Flow*. ESDU. London.

ESDU. (1980). *ESDU 70026: Mean Fluid Forces and Moments on Cylindrical Structures: Polygonal Sections with Rounded Corners Including Elliptical Shapes*. ESDU. London.

FDOT. (2017). *Structures Manual*. Florida Department of Transportation. Tallahassee, Florida.

FDOT. (2015). "Mast Arm Assemblies, Index 17745". *FDOT Design Standards*. Florida Department of Transportation. Tallahassee, Florida.

Harper, Z.S., Edwards, S.T., Consolazio, G.R., Gurley, K.R. (2016). "Drag Coefficients for Construction-Stage Stability Analysis of Bridge Girders Under Wind Loading". *ASCE Journal of Bridge Engineering*. DOI: 10.1061/(ASCE)BE.1943-5592.0000988.

Holmes, J.D. (2007). *Wind Loading of Structures: 2nd Edition*. Taylor & Francis: New York City, NY.

Holmes, J.D. (1996). "Along-wind response of lattice towers – Part II. Aerodynamic damping and deflections". *Engineering Structures*. Vol. 18, No. 7, pp. 483-488.

James, W.D. (1976). *Effects of Reynolds number and Corner Radius on Two-dimensional Flow Around Octagonal, Dodecagonal and Hexdecagonal Cylinders*. Doctoral dissertation, Iowa State University. Ames, Iowa.

Letchford, C., Cruzado, H. (2008). *Risk Assessment Model for Wind-Induced Fatigue Failure of Cantilever Traffic Signal Structures*. Center for Multidisciplinary Research in Transportation Report 0-4586-4. College of Engineering, Texas Tech University. May 2008.

Pulipakaa, N., Sarkarb, P.P., McDonald, J.R. (1998). "On galloping vibration of traffic signal structures", *Journal of Wind Engineering and Industrial Aerodynamics. 77-78*, 327-336. https://doi.org/10.1016/S0167-6105(98)00153-6.

Zdravkovich, M.M., Pridden, D.L. (1977). "Interference between two circular cylinders; Series of unexpected discontinuities". *Journal of Wind Engineering and Industrial Aerodynamics*. Vol. 2, No. 3, pp. 255–270.

Zuo, D., Letchford, C.W. (2010). "Wind-induced vibration of a traffic-signal-support structure with cantilevered tapered circular mast arm". *Journal of Engineering Structures. 32*(10), 3171-3179. https://doi.org/10.1016/j.engstruct.2010.06.005.

Appendix A

This appendix provides FDOT's proposed implementation of C_{di}. This implementation uses a modified hyperbolic representation of C_{di} that is more conservative than the values provided in this study. The hyperbolic fit for C_{di} proposed in this study (Eq. 5) is bounded by [0, 1.2]. FDOT, however, proposes the hyperbolic function (Eq. 5) is increased by a constant factor of approximately 1.1 and bounded by [0.8, 1.2]. The constant factor increases C_{di} such that C_{di} equals the current C_d value used, 1.2, at the maximum value of *h/D*, 11.1, as per attachment dimensions from the state of Florida mast arm inventory. The effect is to normalize the value of C_{di} to the current value of C_d for the most extreme *h/D* ratio in Florida mast arm inventory. Conservatism for the most extreme *h/D* ratio is maintained at current levels while additional conservatism for smaller *h/D* ratios is recognized. In addition, FDOT proposes to limit the minimum value of C_{di} conservatively to 0.8. The resulting FDOT function for C_{di} is given by:

$$C_{di} = \begin{cases} 0.8 & \text{for } \frac{h}{D} \le 1.82 \\ \dfrac{1.2(1.33)\left(\frac{h}{D}\right)^2}{1.2\left(\frac{h}{D}\right)^2 + 1.44\left(\frac{h}{D}\right)} & \text{for } 1.82 < \frac{h}{D} < 11.1 \\ 1.2 & \text{for } \frac{h}{D} \ge 11.1 \end{cases} \quad (8)$$

Figure A-1 illustrates FDOT's proposed implementation of C_{di} (Eq. 8) compared to the hyperbolic fit proposed in this study.

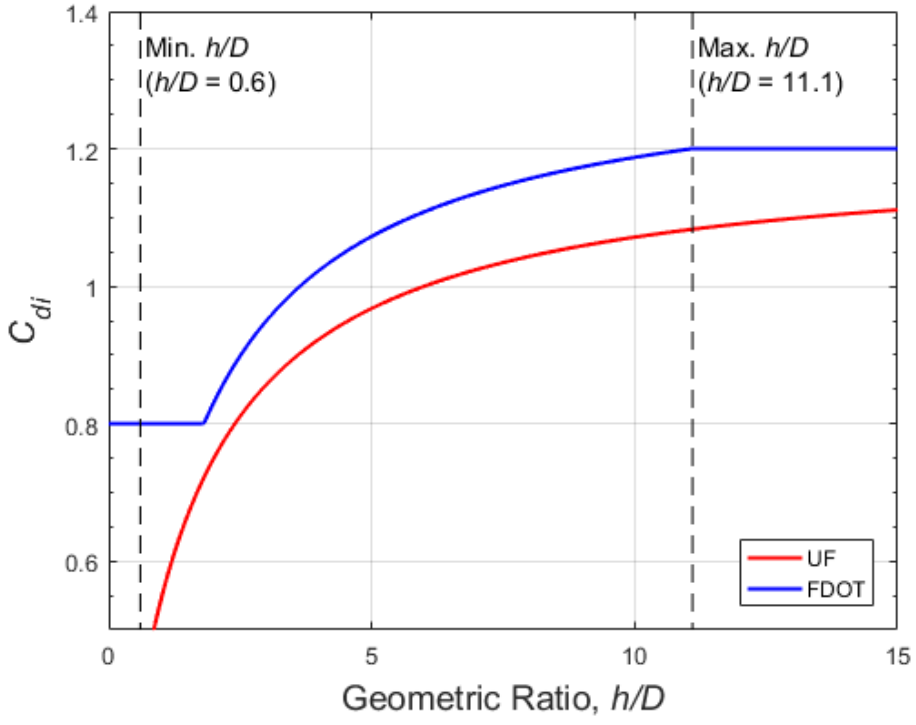

Figure A-1. Proposed hyperbolic fit vs. FDOT's modified hyperbolic fit

Appendix B

As an example of Slotted modification, drawings were generated for the Magnetized Slot modification. This appendix contains an elevation view, side view, and detail drawings of the modification showing key components (i.e., moveable flap, rotational spring, magnet pairs, and hinge). The drawings also illustrate the moveable flaps in the closed, partially open (rotated 45 degrees), and fully open (rotated 90 degrees) positions.

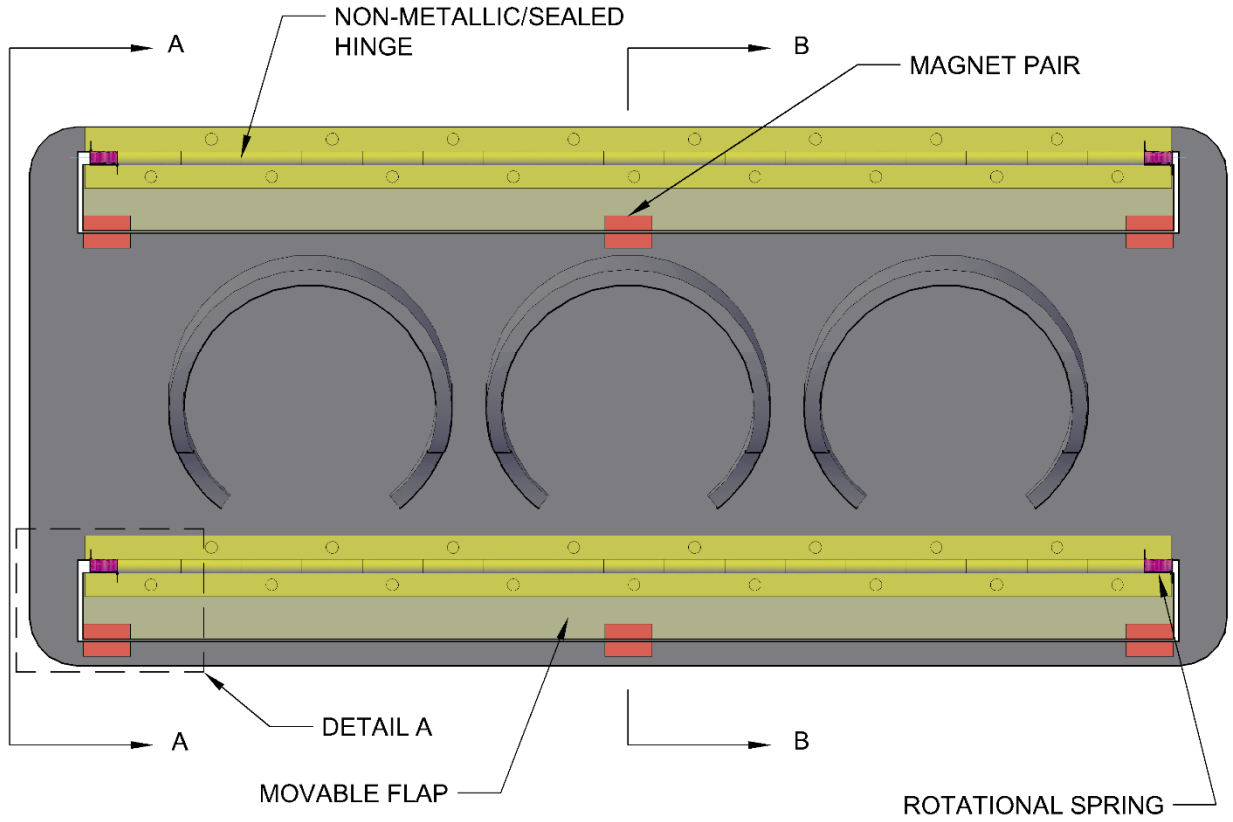

Figure B-1. Plan view of the Magnetized Slot modification

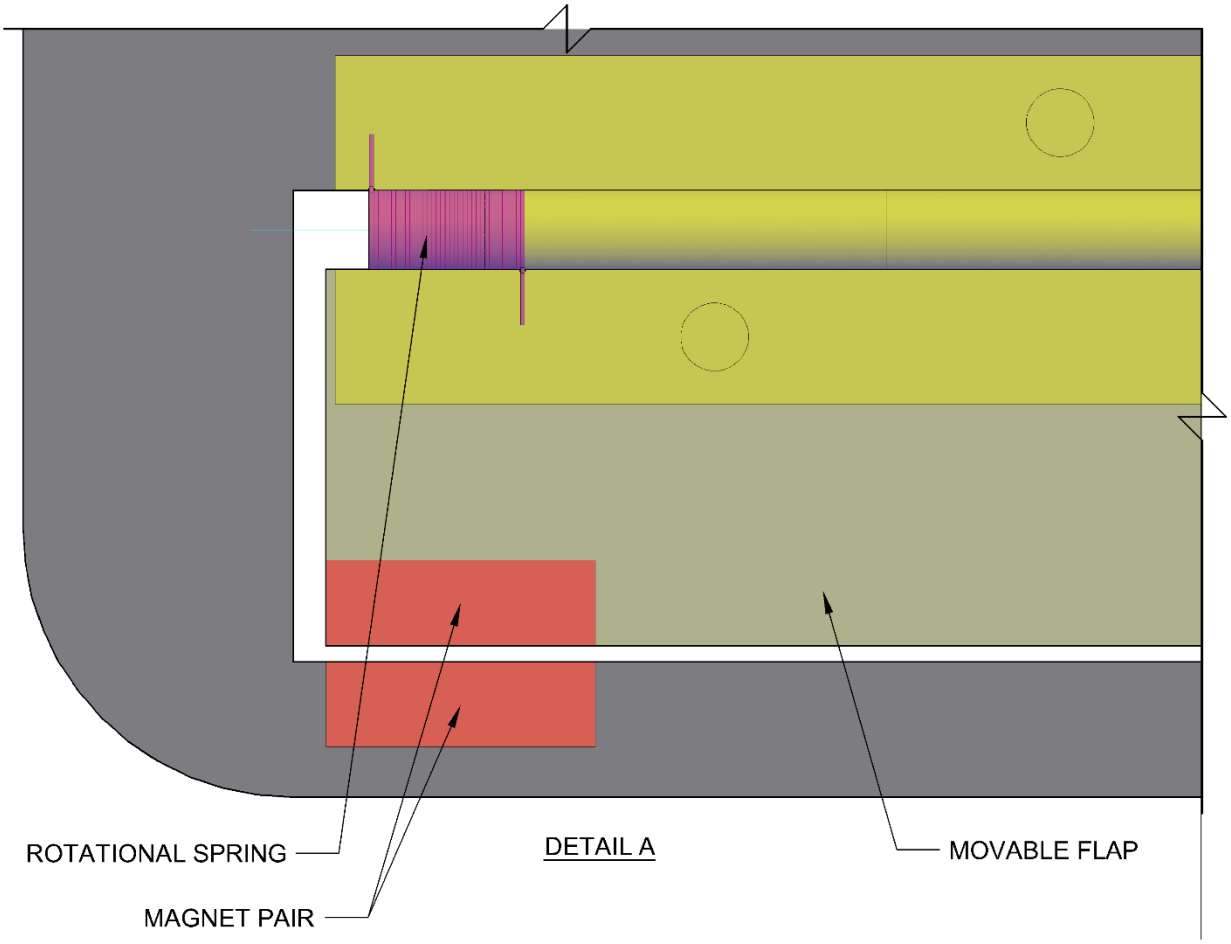

Figure B-2. Detail A, from Plan View, of Magnetized Slot modification

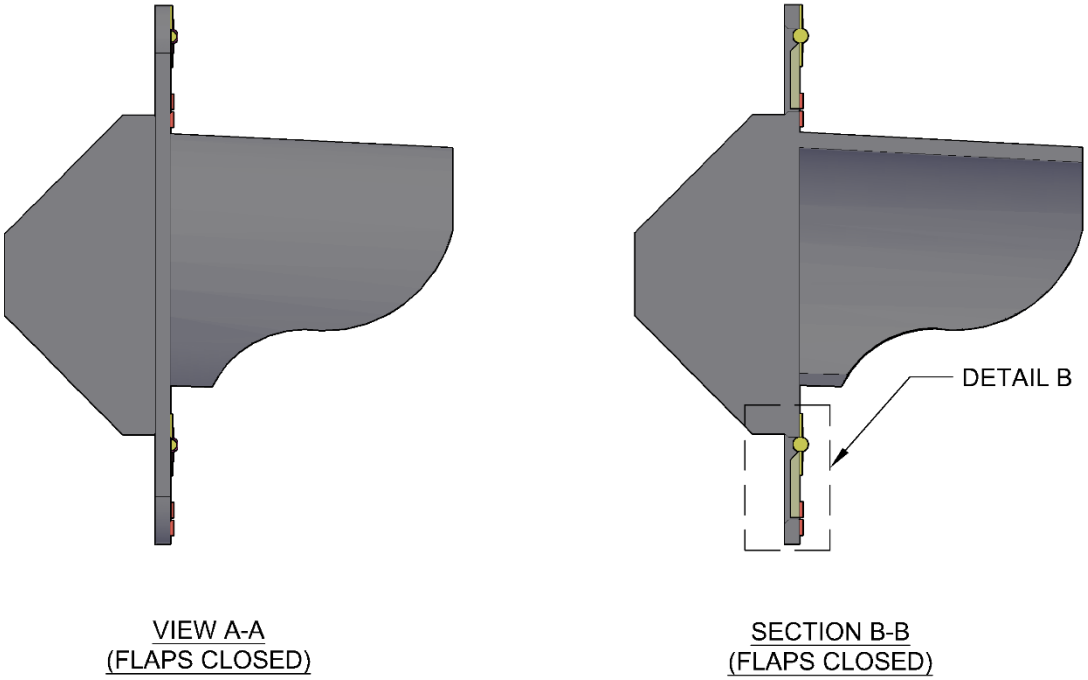

Figure B-3. Side-views of Magnetized Slot modification with flaps closed

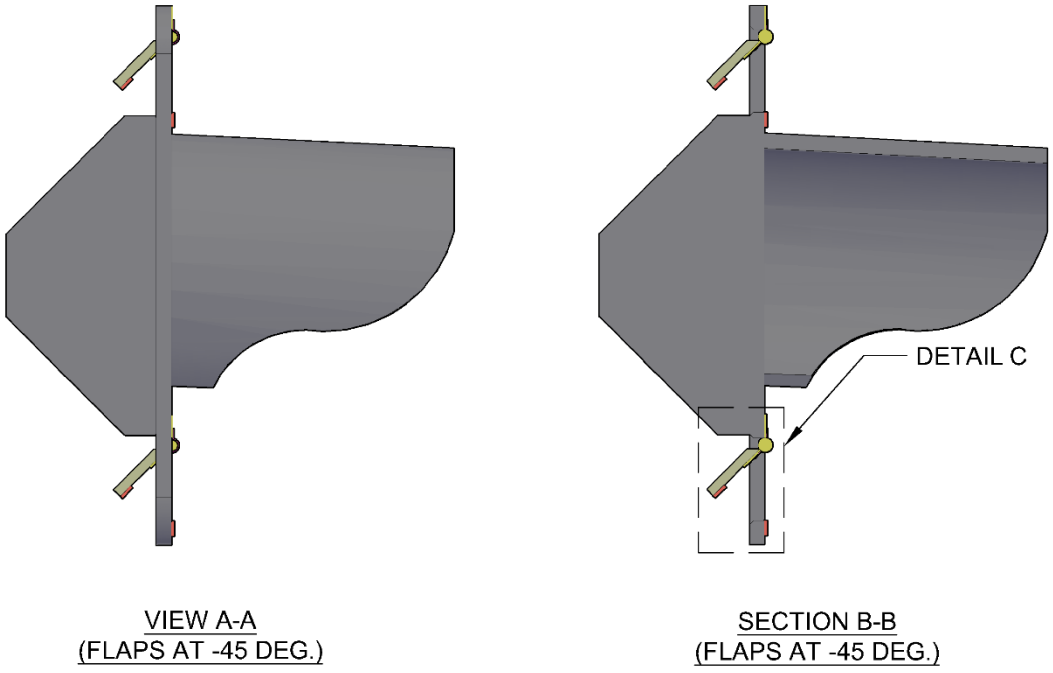

Figure B-4. Side-views of Magnetized Slot modification with flaps opened at -45 degrees

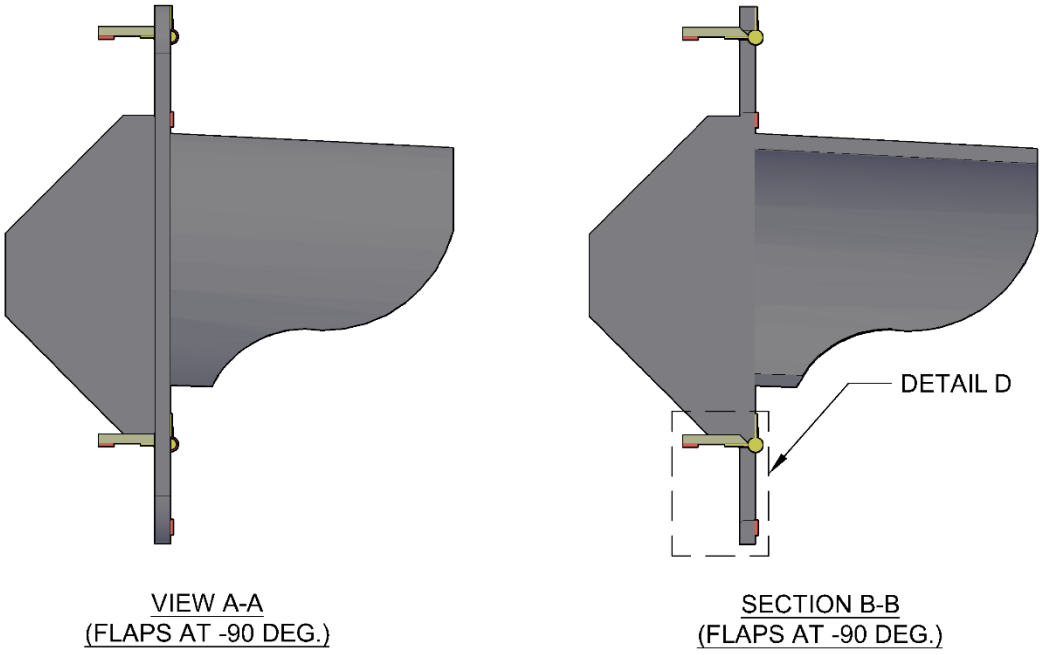

Figure B-5. Side-views of Magnetized Slot modification with flaps opened at -90 degrees

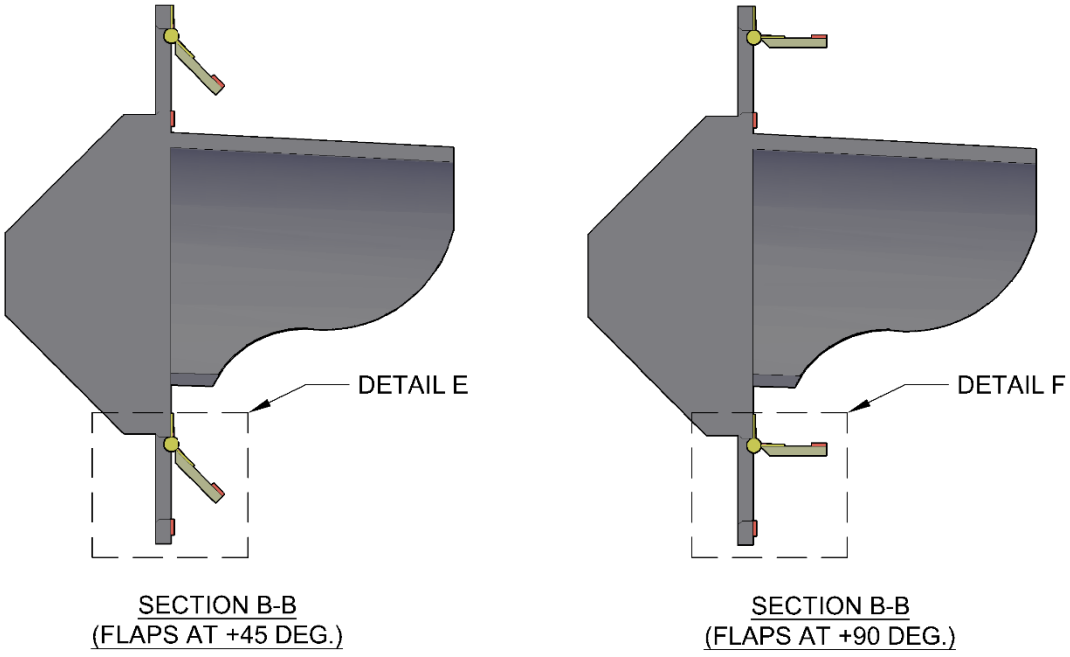

Figure B-6. Side-views of Magnetized Slot modification with flaps opened at +45 degrees and +90 degrees

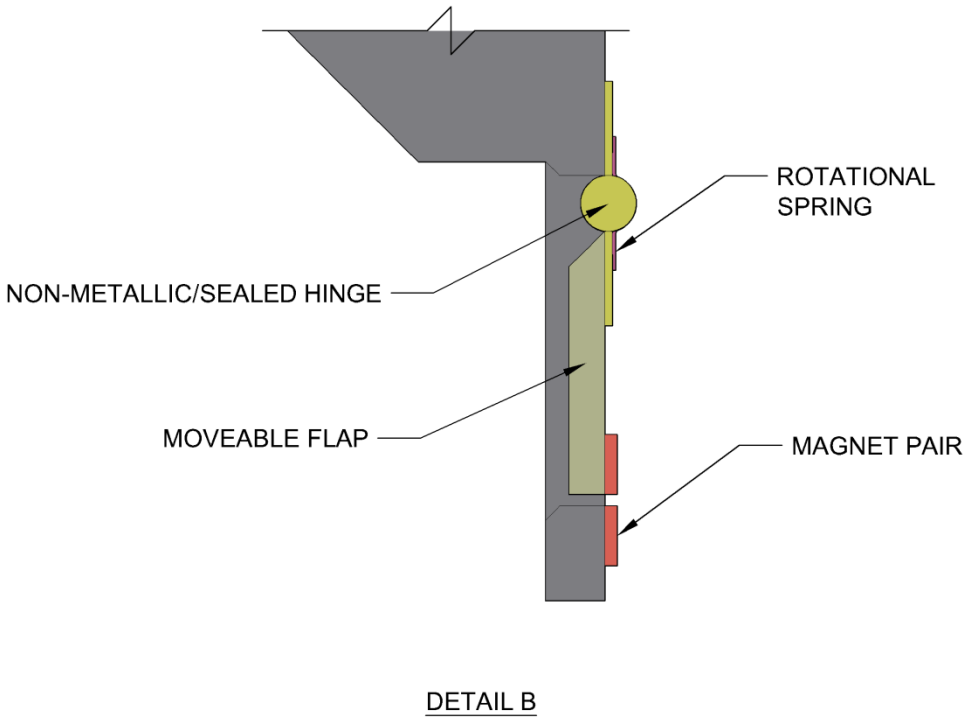

Figure B-7. Detail B, from Plan View, of Magnetized Slot modification

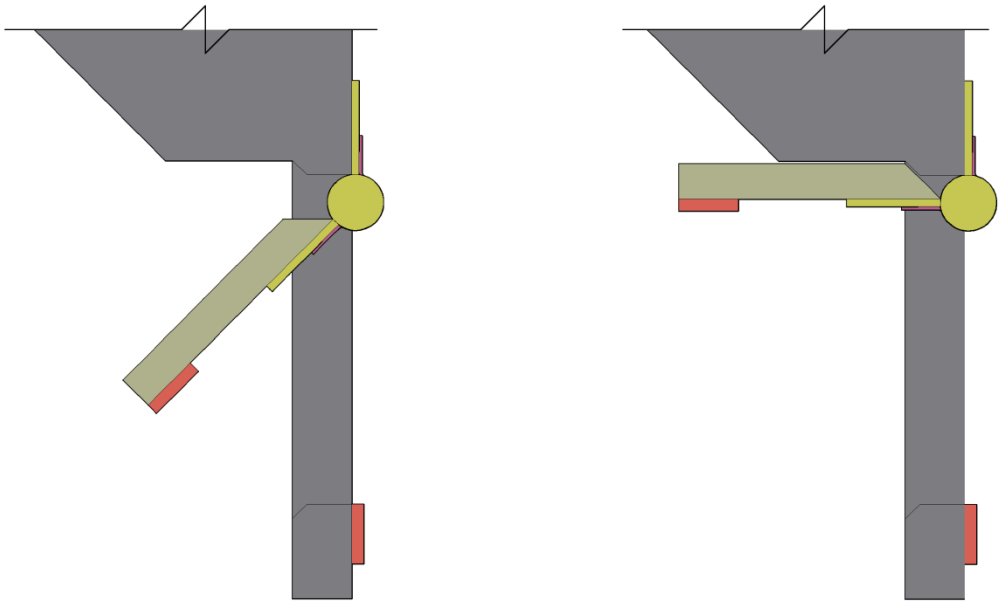

Figure B-8. Detailed side-view drawings of Magnetized Slot modification with flaps opened at -45 degrees, and -90 degrees

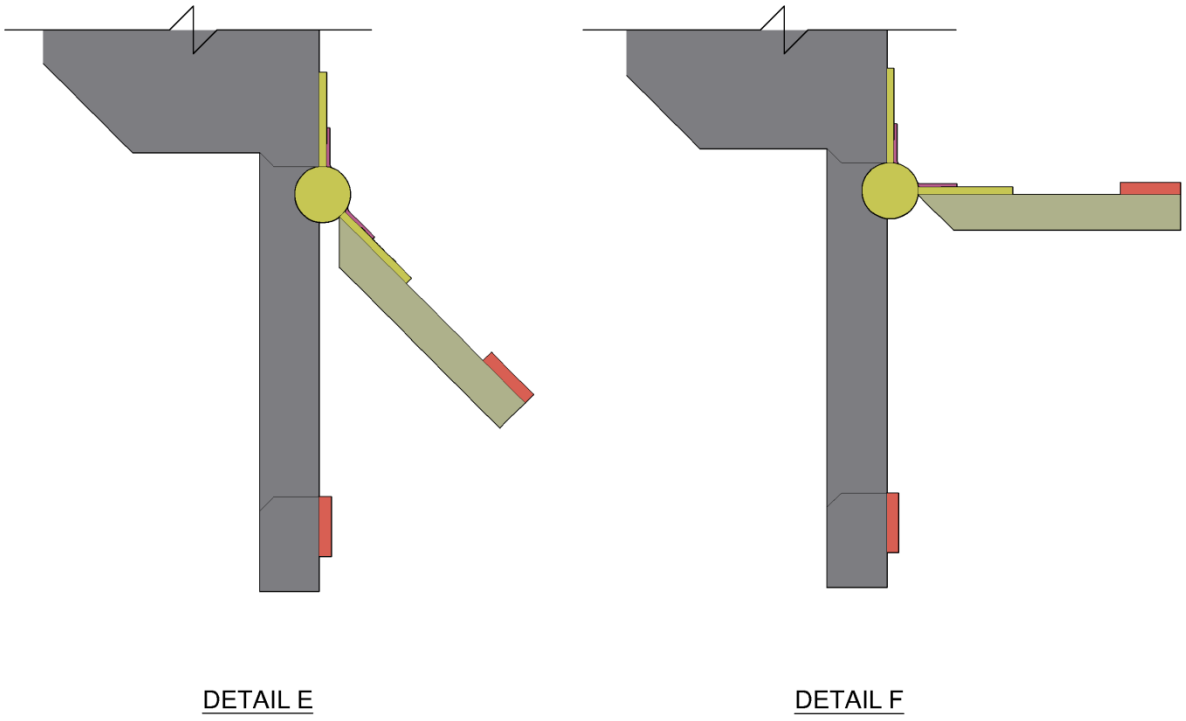

Figure B-9. Detailed side-view drawings of Magnetized Slot modification with flaps opened at +45 degrees, and +90 degrees